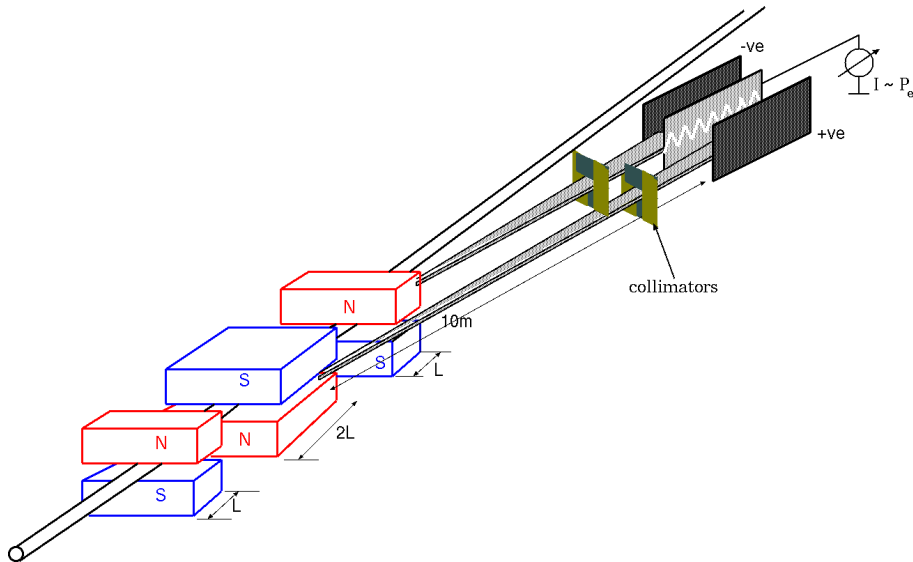


A Novel Spin-Light Polarimeter for the Electron Ion Collider

PRAJWAL MOHANMURTHY



Honors Undergraduate Thesis

Submitted in partial fulfillment of the requirements for the award of the degree of

Bachelor of Science in Physics [Honors]
Department of Physics and Astronomy

Mississippi State University, MS, USA
Nov 25, 2012

1. Reviewer: Dr. Dipankar Dutta

2. Reviewer: Dr. Seth Oppenheimer

3. Reviewer: Dr. Paul Reimer

Day of the defense: Dec 04, 2012

To,
Amma and *Appa*,
for their dedication and admirable way of life.

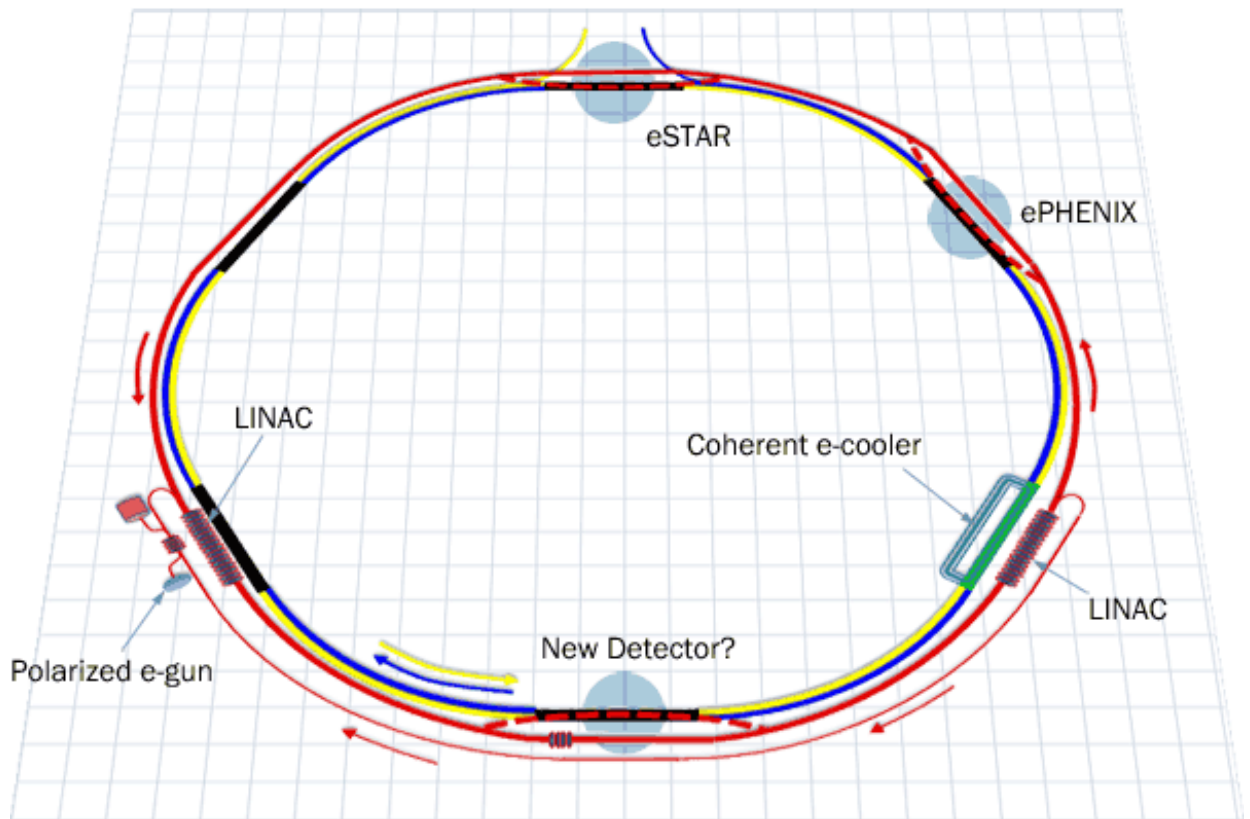
FOREWORD

With Jefferson National Accelerator Facility's (JLAB) 12GeV program in construction phase with a comprehensive set of experiments already planned for the next decade, it is time to think of newer facilities that will further push the boundaries and continue the mission of a premier nuclear physics laboratory to explore the frontiers of fundamental symmetries and nature of nuclear matter. Building of an Electron Ion Collider (EIC) seems to be a natural future step. JLAB is a fixed target laboratory, but at the EIC, the target will also be accelerated thereby providing access to precision physics of quarks and gluons at much higher energies (than 12GeV). JLAB mainly consists of the Continuous Electron Beam Accelerator and 3 halls where the fixed target experiments are performed. Brookhaven mainly consists of the Relativistic Heavy Ion Collider with a number of main collision points on the beam line. There have been two leading proposals for the EIC, *i.e.*

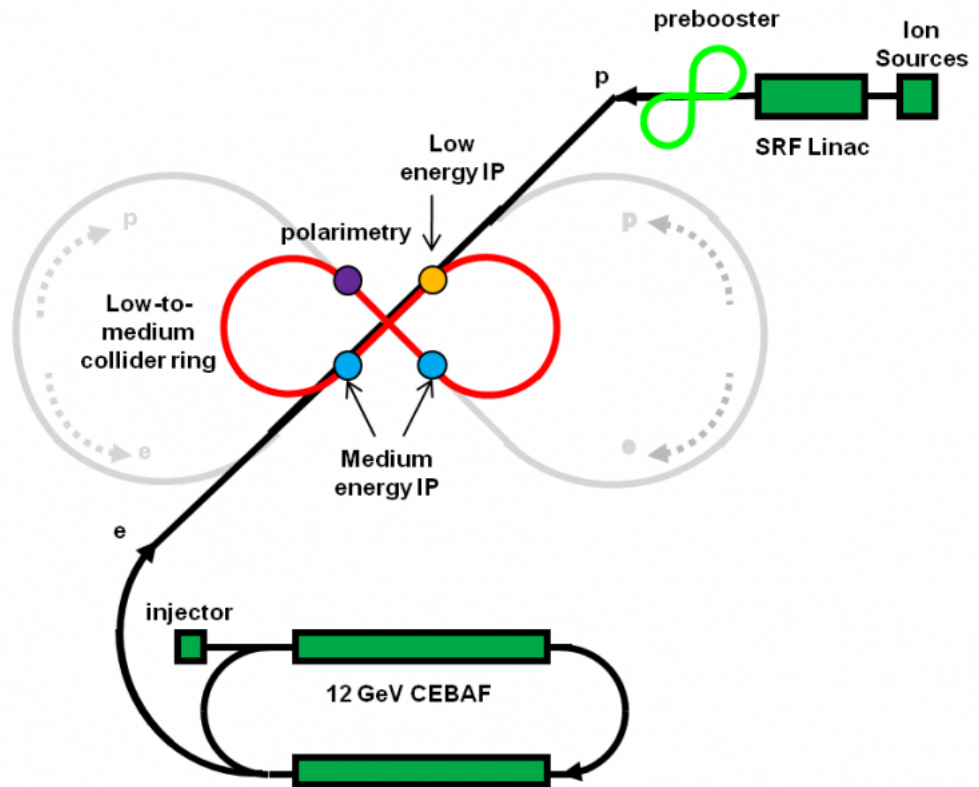
- **eRHIC** : Electron - Relativistic Electron Collider @ Brookhaven National Laboratory, Upton, NY ^[i]

^[i]eRHIC: High Energy Electron-Ion collider,
<http://www.bnl.gov/cad/eRhc/>,
Retrieved on: Nov 25, 2011

^[ii]ELIC: Electron Light Ion Collider at CEBAF,
<http://casa.jlab.org/research/elic/elic.shtml>,
Retrieved on: Nov 25, 2011



- **ELIC** : Electron - Light Ion Collider @ Jefferson National Accelerator Laboratory, *Newport News, VA* ^[ii]



Brookhaven already has an ion accelerator and the eRHIC would need addition of an electron accelerator, whereas JLAB already has the electron accelerator and the ELIC would need addition of an ion accelerator.

At JLAB, polarization of the electron beam has played a vital role a number of experiments such as the PVDIS (Parity Violating Deep Inelastic Scattering) and the QWeak (which measured the weak charge of proton). To measure the polarization of the electron beam, JLAB has commissioned Compton and Møller polarimeters which have met the precision demands of JLAB, but the Møller Polarimeter generates a large background as it uses ee scattering to measure the polarization. The future demands greater precision in the measurement of polarization of the beam and so at the EIC, it would be convenient to have a second non-invasive polarimeter, besides a Compton Polarimeter, for systematics comparison.

ABSTRACT

A novel precision polarimeter will go a long way in satisfying the requirements of the precision experiments being planned for a future facility such as the Electron Ion Collider. A polarimeter based on the asymmetry in the spacial distribution of the spin light component of synchrotron radiation will make for a fine addition to the existing-conventional Møller and Compton polarimeters. The spin light polarimeter consists of a set of wiggler magnet along the beam that generate synchrotron radiation. The spacial distribution of synchrotron radiation will be measured by an ionization chamber after being collimated. The up-down spacial asymmetry in the transverse plane is used to quantify the polarization of the beam. As a part of the design process, firstly, a rough calculation was drawn out to establish the validity of such an idea. Secondly, the fringe fields of the wiggler magnet was simulated using a 2-D magnetic field simulation toolkit called Poisson Superfish, which is maintained by Los Alamos National Laboratory. This was used to account for beam motion effects and the corresponding correlations were show to be negligible. Lastly, a full fledged GEANT-4 simulation was built to study the response time of the ionization chamber. This GEANT-4 simulation was analyzed for variety of effects that may hinder precision polarimetry. It was found that a Spin-Light Polarimeter would be a fine relative polarimeter.

ACKNOWLEDGEMENTS

This work has been generously supported by Jefferson Science Associates, LLC - Undergraduate Fellowship Program at Thomas Jefferson National Accelerator Facility, VA, USA.

Additional, but substantial, funding has been provided by the Mississippi State Consortium, MS, USA, and the Office of Research & Economic Development, MS, USA. Travel funds has also been provided by the Shackouls Honors College, MS, USA, The Conference Experience for Undergraduates program of the American Physical Society's Division of Nuclear Physics, USA, and the Graduate School of Mississippi State University, MS, USA.

Thanks are due to the Department of Physics and Astronomy at Mississippi State University, MS, USA for providing office & lab space and also the computational infrastructure required for this computational intensive work.

It would have been impossible to quickly adapt the GEANT4 code to the latest standards without the express support from Edward 'Jed' Legget, a graduate student in the Medium Energy Physics Group at Mississippi State University, MS, USA.

The author would also like to extend his gratitude to the Hall-A Compton group at Jefferson Lab, VA, USA, especially Dr. Gregg Franklin of Carnegie Mellon University, PA, USA for providing the basic Hall-A Compton chicane magnets' LANL Poisson codes.

Most importantly, thanks are due to Dr. Dipankar Dutta, who has been relentlessly at work on this project, guiding and helping the effort at every step as the major advisor and supervisor in charge.

Last, but not least, the author likes to thank the thesis defense committee members Dr. Paul Reimer of Argonne National Laboratory, IL, USA and Dr. Seth Oppenheimer of the Shackouls Honors College, MS, USA for their very thoughtful inputs.

CONTENTS

I	GROUND WORK	1
1	THEORY	3
1.1	Classical SR-Power Law	3
1.2	Quantum Corrections	4
1.3	Spin - Light	6
2	INITIAL DESIGN	7
2.1	Wiggler Magnet	7
2.2	Collimator	8
2.3	Ionization Chambers	8
II	PROJECT WORK	11
3	DESIGN CONSIDERATIONS	13
3.1	Spin - Light Characteristics	13
3.2	Wiggler Magnet	14
3.2.1	Effects of wiggler on the beam	16
3.2.2	Effects of realistic dipole magnetic field with fringes	17
3.3	Collimation and Spin-Light fan size	19
3.4	Ionization Chambers	20
3.4.1	Relative Polarimetry	21
3.4.2	Absolute Polarimetry	25
3.4.3	Effects of Extended Beam Size	28
4	GEANT4 SIMULATIONS	31
4.1	Spin Light in Geant4 and Asymmetry	33
4.2	Synchrotron Light Profile at the Ionization Chambers and Collimation	35
5	SUMMARY	39
5.1	Systematics	39
5.2	Conclusion and Future Work	40
A	LISTS AND PERMISSIONS	41
A.1	List of Figures	41
A.2	List of Referenced Publications	42
A.3	License	43
B	ESSENTIAL CODES	45
B.1	Numerical Integration of the SR - Power Law	45
B.2	LANL Poisson SupeFish Geometry Description	58
B.3	Recursive SR Spectra Adding Code	60
B.4	GEANT4 Geometry File	63
B.5	GEANT4 Stacking Action File	83

Part I

GROUND WORK

Initial work at proposal time is discussed here. Also included are some glimpses into the theory that motivates this work. This section enumerates the work borrowed from previous work done in this field notably at Novosibirsk, Russia. Also presented are some recent developments in Ionization Chamber Technology.

THEORY

1.1 CLASSICAL SR-POWER LAW

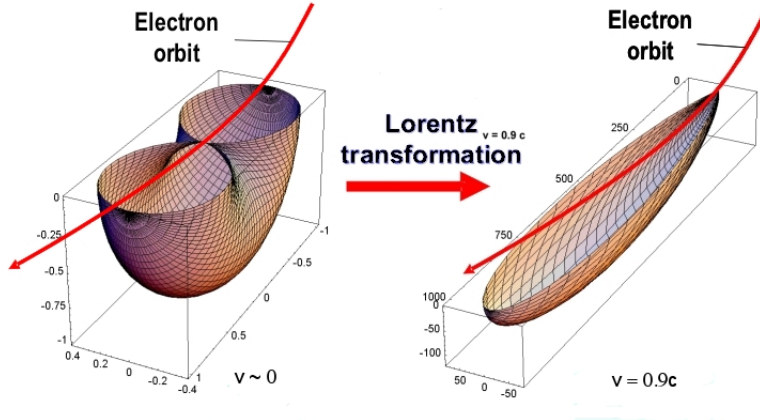


Figure 1: Angular distribution of synchrotron radiation shown for the bottom half of the electron's orbital plane. The left figure is for slow electrons, $\beta \sim 0$ and the right figure is for highly relativistic electrons, $\beta \sim 1$. [1]

The total radiative power due to circularly accelerated particles is given by Larmor formula which is $P_{\text{clas}} = \frac{2}{3} \frac{e^2 \gamma^4 c}{R^2}$ (i.e. P is proportional to E^4) [here P_{clas} is the classical total radiative power, e is the electron charge, $\gamma = \frac{E}{m_e c^2}$: the Lorentz boost, c is the speed of light, and R is the radius of trajectory of the electrons]. The angular dependence of radiative power can also be computed via classical electromagnetism.

$$\frac{dP_{\text{clas}}}{d\Omega} = \frac{e^2 \gamma^4 c}{4\pi R^2} \frac{(1 - \beta \cos\theta)^2 - (1 - \beta^2) \sin^2\theta \cos^2\phi}{(1 - \beta \cos\theta)^5} \quad (1)$$

In classical electrodynamics the angular distribution of radiative power from synchrotron (SR) light can be calculated, as indicated in the above eq.(1) [2] [where $d\Omega = d\theta d\phi$, and $\beta = \frac{\text{speed of particle}}{\text{speed of light}}$]. The SR light-cone is spread over a well defined cone with the angular spread - θ in retarded time $\Delta t' \approx \frac{\Delta\theta}{\omega_0}$ [where ω_0 is the angular frequency of the photon]. There is no reason to believe that the SR spectrum is mono-energetic. The spectral width of SR radiation can be formulated: $\Delta\omega \approx \frac{1}{\Delta t'(1-\beta)} = \frac{1}{2\gamma^3 \omega_0}$. A critical acceleration can be envisioned at which the SR may consist of just 1 photon by

[1] Proposal to the EIC R & D: https://wiki.bnl.gov/conferences/images/7/74/RD2012-11_Dutta_eic_polarimetry.pdf

[2] D. D. Ivanenko, I. Pomeranchuk, Ya Zh. Eksp. Teor. Fiz. 16, 370 (1946); J. Schwinger, Phys. Rev. 75, 1912 (1947)

[3] I. M. Ternov and V. A. Bordovitsyn, Vestn. Mosk. Univ. Ser. Fiz. Astr. 24, 69 (1983); V. A. Bordovitsyn and V. V. Telushkin, Nucl. Inst. and Meth. B266, 3708 (2008)

solving the equation $\gamma m_e c^2 = \hbar \omega_C$. To achieve this acceleration, a critical uniform magnetic field can be applied on an electron which is $B_c = \frac{m_e^2 c^3}{e \hbar}$ [here m_e refers to the rest mass of an electron]. The energy of the electron at these accelerations can be called the critical energy, $E_C = m_e c^2 \sqrt{\frac{m_e R_c}{\hbar}} \approx 10^3 \text{ TeV}$ for R_c of about 10m. It is important to note that even though accelerated electron is under consideration, the equations above don't have acceleration terms. This is because a conventional circular motion is used to calculate the parameters and only the speed is important as the acceleration is a function of speed.

1.2 QUANTUM CORRECTIONS

In the classical theory, the spin does not explicitly appear in the equation. But, in QED, the angular dependence of synchrotron (SR) light can be calculated to a great degree of precision and the spin of the electron involved in SR emission appears explicitly in the power law [3]. The quantum power law for SR was worked out by Sokolov, Ternov and Klepikov as a solution to the Dirac equation [4] and includes the effects introduced by electrons undergoing $j \rightarrow j'$ (spin dependence) transitions besides also elaborating on the fluctuations to the electron orbit ($n \rightarrow n'$ transitions - linear correction to orbit and $s \rightarrow s'$ transitions - quadratic correction to orbit). The power law when integrated over all polarizations and (spacial) angular dependencies, can be written as [5];

$$P = P_{\text{Class}} \frac{9\sqrt{3}}{16\pi} \sum_s \int_0^\infty \frac{y dy}{(1+\xi y)^4} I_{ss'}^2(x) F(y) \quad (2)$$

$$F(y) = \frac{1+jj'}{2} \left[2(1+\xi y) \int_y^\infty K_{\frac{2}{3}}(x) dx + \frac{1}{2} \xi^2 y^2 K_{\frac{2}{3}}(y) - j(2+\xi y) \xi y K_{\frac{1}{3}}(y) \right] \\ + \frac{1-jj'}{2} \xi^2 y^2 \left[K_{\frac{2}{3}}(y) + 1 K_{\frac{1}{3}}(y) \right] \quad (3)$$

{Where $\xi = \frac{3B}{2B_c} \gamma$, ' j ' is the spin of the electron, $y = \frac{\omega_e}{\omega_c}$, $x = \frac{3}{4} \frac{\xi \gamma^3 y^2}{(1+\xi y)^2}$, $I_{ss'}(x)$ are Laguerre functions, and $K_n(x)$ are modified Bessel functions}.

If $\xi \ll 1$ (given $B_c \approx 4.41 \times 10^9$ Tesla) then Eq. (3) can be Taylor expanded in terms of powers of ξ as follows;

$$P = P_{\text{class}} \left[\left(1 - \frac{55\sqrt{3}}{24} \xi + \frac{64}{3} \xi^2 \right) - \left(\frac{1+jj'}{2} \right) \left(j\xi + \frac{5}{9} \xi^2 + \frac{245\sqrt{3}}{48} j\xi^2 \right) \right. \\ \left. + \left(\frac{1-jj'}{2} \right) \left(\frac{4}{3} \xi^2 + \frac{315\sqrt{3}}{432} j\xi^2 \right) + \dots \right] \quad (4)$$

Eq. (3) and (4) include the a number of effects;

[4] A. A. Sokolov, N. P. Klepikov and I. M. Ternov, *JETF* 23, 632 (1952).

[5] A. A. Sokolov and I. M. Ternov, *Radiation from Relativistic Electrons, A.I.P. Translation Series, New York (1986)*; I. M. Ternov, *Physics - Uspekhi* 38, 409 (1995).

- Classical SR
- Thomas Precession
- Larmor Precession
- Interference between Larmor and Thomas Precession
- Radiation from intrinsic magnetic moment (including anomalous magnetic moment)

Eq. (4) can be re-expressed as a difference between power from unpolarized and polarized electron beam.

$$P_{Spin} = P_{Pol.} - P_{UnPol.} = -j\xi P_{Clas} \int_0^\infty \frac{9\sqrt{3}}{8\pi} y^2 K_{\frac{1}{3}}(y) dy \quad (5)$$

Eq. (5) is essentially the spin light that this project is based on which opens up the possibility of using SR part to measure the polarization of the beam.

The power law in eq. (5), that was derived using QED, has been extensively tested and verified at the Novosibirsk Storage ring over a large range of wavelengths (of SR). For this, the Novosibirsk group used a "snake" shaped wiggler magnet to produce the SR from a relatively low energy electron beam of about 0.5GeV@100μA.

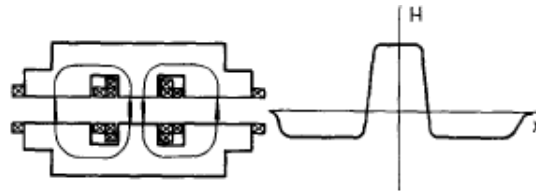


Fig. 1. The field vs the current in the 'snake'. A schematic of the 'snake' and the field distribution along its axis are shown below.

Figure 2: Magnetic snake used at the VEPP-4 as a source of SR to test the spin dependence of SR. [6]

Figure 3, clearly demonstrated the power dependence of the SR on beam-electron polarization. It remains to be shows as to how the SR spectra could be measured.

The spin flip probability has a special significance in modern day electron storage rings and is given by the relation [4];

$$W_{\uparrow\downarrow} = \frac{1}{\tau} \left(1 + j \frac{8\sqrt{3}}{15} \right) \quad (6)$$

{where $j = +1$ is spin along the magnetic field (and $j = -1$ is spin against magnetic field), and τ is the time involved in the process}.

As a result of the probability of spin aligning with the magnetic field direction would become very high over long periods of time. A circulating electron beam, such as ones in storage rings self polarize,

[5] S. A. Belomesthnykh et al., Nucl. Inst. and Meth. 227, 173 (1984).

[6] K. Sato, J. of Synchrotron Rad., 8, 378 (2001).

[7] J. Le Duff, P. C. Marin, J. L. Manson, and M. Sommev, Orsay - Rapport Technique, 4-73 (1973).

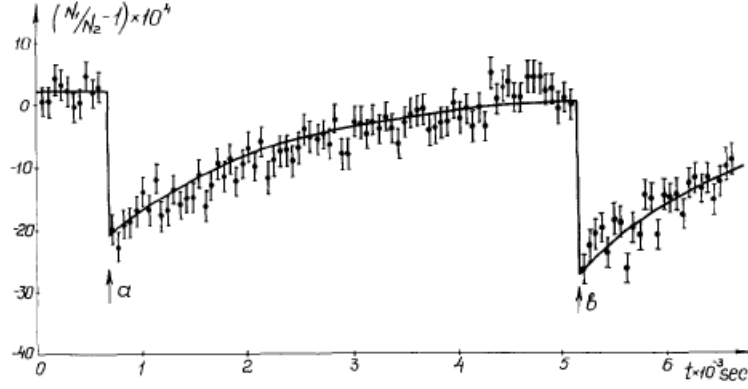


Fig. 12. The measurement results of the SR-intensity as a function of the degree of polarization of the beam. The field in the 'snake' coincides, in direction, with the storage ring guiding field. At points a and b one of the bunches (N_1), was quickly depolarized. The measurement time at a point is 60 s. The bunch polarization time is $\tau_p = 1740 \pm 20$ s ($\xi = 0.726$).

Figure 3: Results from the experiment showing the increase in intensity of SR as the polarization builds up and then suddenly drops to zero when an RF field is used to depolarize the beam. [6]

and this has been studied in great detail at many storage rings such as ones at DESY, PSI and CESR though it was first observed at the Orsay storage ring [7].

1.3 SPIN - LIGHT

In the Spin-Light polarimeter, the spin-flip term in the power law does not play an important role. The integral power law without the spin-flip term can be written as [4];

$$P_\gamma = \frac{9\eta_e}{16\pi^3} \frac{ce^2}{R^2} \gamma^5 \int_0^{\text{inf}} \frac{y^2 dy}{(1 + \xi y)^4} \oint d\Omega (1 + \alpha^2)^2 \times \left[K_{\frac{2}{3}}^2(z) + \frac{\alpha^2}{1 + \alpha^2} K_{\frac{1}{3}}^2(z) + j\xi y \frac{\alpha}{\sqrt{1 + \alpha^2}} K_{\frac{1}{3}}(z) K_{\frac{2}{3}}(z) \right] \quad (7)$$

where $z = \frac{\omega}{2\omega_c} (1 + \alpha^2)^{\frac{2}{3}}$ and $\alpha = \gamma\psi$ where ψ is the vertical angle *i.e.* above and below the orbit of the electron. Notice that the last term with a j disappears from the integral over all angles ($-\frac{\pi}{2} \leq \psi \leq \frac{\pi}{2}$). But for an electron that is polarized, the power below (*i.e.* $-\frac{\pi}{2} \leq \psi \leq 0$) and above (*i.e.* $-\frac{\pi}{2} \leq \psi \leq \frac{\pi}{2}$) are spin dependent. More importantly the difference between the power radiated above and power radiated below is directly spin dependent, which can be directly obtained from Eq. (7) in differential form for circular arcs in the circular cross-section the SR-light cone at an angle θ .

$$\frac{\Delta P_\gamma(j)}{\Delta\theta} = \frac{3}{2} \frac{\hbar c \gamma^3 y}{R} \times \frac{3}{\pi^2} \frac{1}{137} \frac{I_e}{e} j\xi\gamma \int_{y_1}^{y_2} y^2 dy \int_0^\alpha \alpha (1 + \alpha^2)^{\frac{2}{3}} K_{\frac{1}{3}}(z) K_{\frac{2}{3}}(z) d\alpha \quad (8)$$

INITIAL DESIGN

It is obvious now that our setup will have a wiggler magnet which shall be the source of SR and an ionization chamber to measure the power spectra of the SR emitted at the wiggler magnet by the polarized electrons.

2.1 WIGGLER MAGNET

In order to create a fan of SR light (as illustrated in Figure 5), the electron beam could be made to bend in presence of a magnet. An arrangement that would lead to the production of the SR-Cone must look similar to the "snake" magnets that were used by VEPP-4 as described in *Chapter 1*.

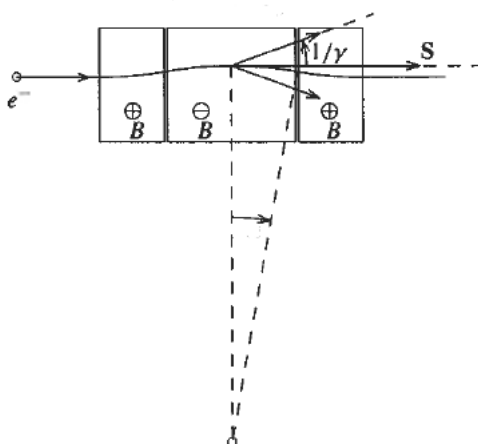


Figure 4: A 3-pole wiggler with central dipole twice the length of end dipoles.

A set of 3 dipoles (3 - pole dipole), each with constant uniform magnetic field would be ideal for this purpose. The central dipole would have twice the pole length as compared to the ones on either side of the central dipole, but with a magnetic field an opposite polarity like in Figure 4. This design will give rise to 4 fans, 2 towards either side of the beam (left and right). Each of the fan will have spacial asymmetry as a function of spin - polarization of the electrons in the vertical plane (up - down the electron beam's orbit which is perpendicular to the plane which contains the 4 fans). The 4 fans help characterize the systematics better since this configuration will flip the sign of the

spin - dependent term in Eq. (8) twice essentially returning the sign to the original status.

With this geometry in mind, one could then simulate and calculate the requisite pole strengths and pole lengths appropriate to energies at Electron Ion Collider (EIC). Of course, one would also have to consider time scales at which the statistics would be sufficient to achieve the design requirement ($< 1\%$) of precision. A number of techniques were employed to tackle the above issues. Including issues such as optimizing the distance between each pole were solved through a full fledged GEANT-4 simulation.

2.2 COLLIMATOR

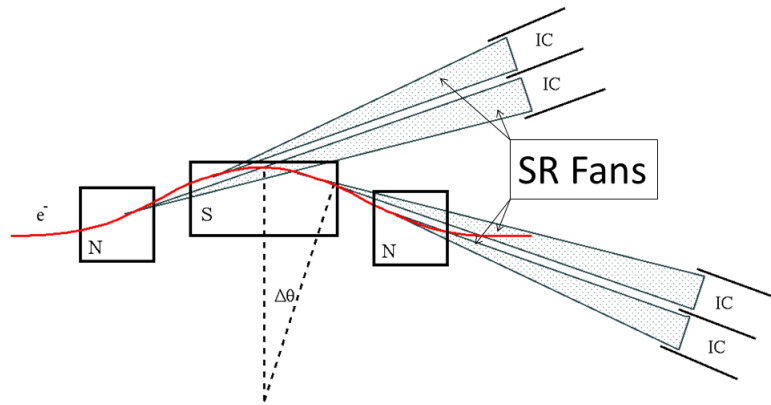


Figure 5: A rough schematic of the 4 fans that shall be created by the Wiggler Magnet

The 4 fans of SR-Light need not be separated from each other. They may in fact overlap and extracting the power - asymmetry information from complicated overlappings would require extensive modeling. This might also introduce new sources of uncertainties. Therefore to uniquely sample each fan at the ionization chamber, collimators would need to be placed on each face of the dipoles to direct and separate the fans of SR. The position of the collimators will be calculated using optimized values of pole - strengths, pole - lengths and relative position of each of the dipoles.

2.3 IONIZATION CHAMBERS

The Ionization Chambers (IC), one on each side (2 fans per IC) of the beam, could be used for measuring the spacial asymmetry in the SR - fans to be used to compute the polarization of the electrons in the beam. One would not expect a large asymmetry in the Spin-Light component (of the order of about 10^{-4}), therefore a high resolution, low noise IC is demanded. The IC will be very close to the

beam line and the spin-independent background may be as high as 10^{12} photons/s, therefore the ICs have to be radiation hard. The geometry of the magnets could be changed to deal with SR Spectra with characteristic energy peak in the ranges of about 500keV – 2.5MeV. An IC with Xenon as ionization media operated in the current mode can in principle handle high fluxes and have low noise disturbances [8]. It might be important to note that the Spin-Light asymmetry is spread over the entire spectra of the SR. Sampling radiation over large energy spectrum becomes important. Since Xenon has the lowest ionization energy of about 21.9eV, among non-radioactive noble gases, it seems to be an ideal candidate. ICs with Xenon under high pressures have already been developed and well tested to perform well in the energy ranges of 50keV – 2.0MeV [9]. Pressures involved in HPXe ICs exceed 50atm@0.55g/cc but they work well at room-temperature [10],[11],[12]. One of the bottlenecks was the precision of purity of the Xenon gas in its pristine form. But owing to advances in gas purification techniques [13], a best energy resolution of 2.4% at about 0.662MeV has been shown to be possible when current signals from the shower is used in presence of prompt Xenon scintillation [14]. The results from this attempt has been fairly promising (Figure 6). ICs with 3% – 4% energy resolution are even being sold commercially by PROPORTIONAL TECHNOLOGIES INC. [15].

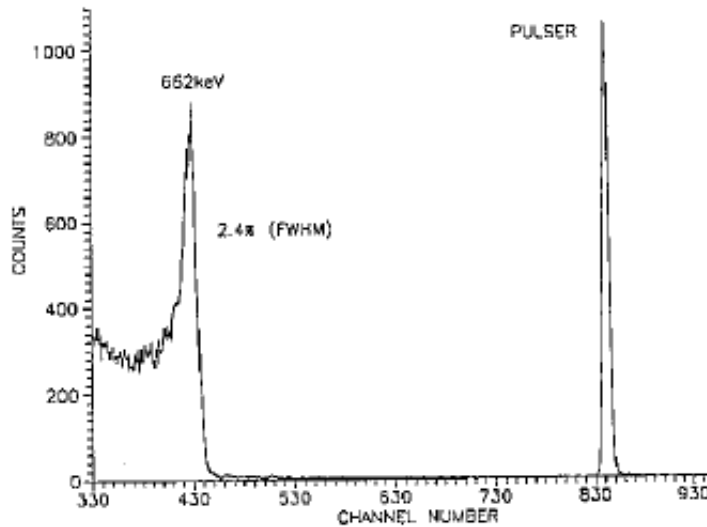


Figure 6: Cs¹³⁷: $E_i = 1.7\text{kV/cm}$, pulse height spectrum in 57atm at 295K of xenon, $E_i = 1.7\text{kV/cm}$ [14].

[8] A. E. Bolotnikov and B. Ramsey, *Nucl. Inst. and Meth.* A396, 360 (1997).

[9] T. Doke, *Portugal Phys.* 12, 9 (1981).

[10] V. V. Dmitrenko et al., *Sov. Phys.-tech. Phys.* 28, 1440 (1983); A. E. Bolotnikov et al., *Sov. Phys.-Tech. Phys.* 33, 449 (1988)

[11] C. Levin et al., *Nucl. Inst. and Meth.* A332, 206 (1993).

[12] G. Tepper and J. Losee, *Nucl. Inst. and Meth.* A356, 339 (1995).

[13] A. E. Bolotnikov and B. Ramsey, *Nucl. Inst. and Meth.* A383, 619 (1996).

[14] G. Tepper and J. Losee, *Nucl. Inst. and Meth.* A368, 862 (1996).

[15] Proportional Technologies Inc., www.proportionaltech.com.

Part II

PROJECT WORK

In this section, the work is presented with additional studies resulting from discussion with experts. It includes establishing the idea with a "back of the envelop calculation" backed by a full fledged GEANT-4 simulation. Also, related effects such as beam motion were studied and their effects that impact the polarimeter negatively were shown to be minimal. Even though the GEANT-4 simulation is still in the making, a skeletal code is briefly explained here.

DESIGN CONSIDERATIONS

3.1 SPIN - LIGHT CHARACTERISTICS

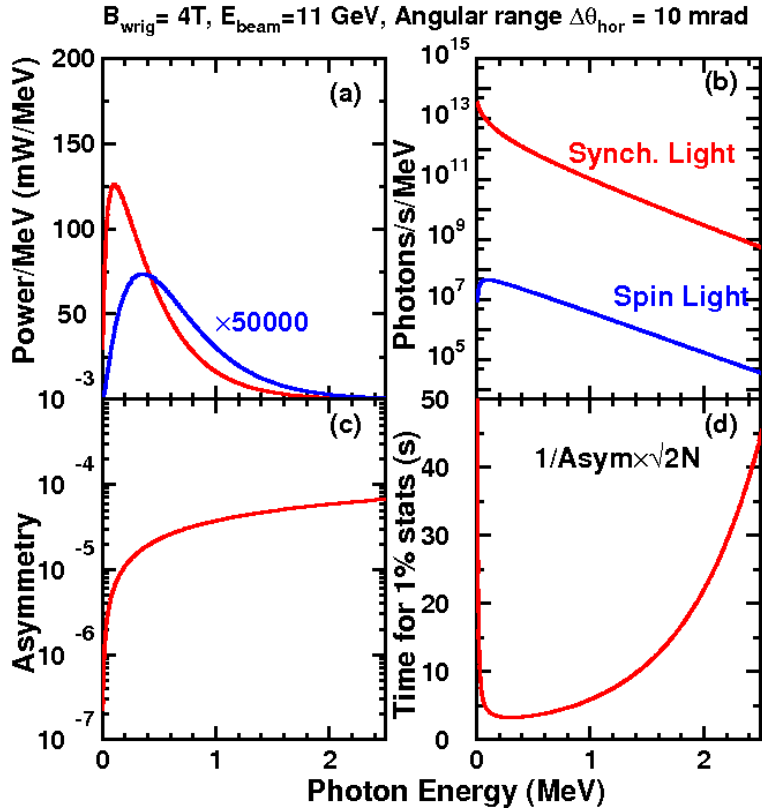


Figure 7: A. Plot of difference between the number of SR and spin light photons that go above and below the orbit of the electron (ΔP_γ) vs. their energy
 B. Plot of total number of SR, spin light photons P_γ vs. their energy
 C. Plot of the Asymmetry vs. the photon energies
 D. Plot of time required to achieve 1% statistics by sampling one wavelength of the spin-light spectra vs. the energy of the photons.

The spin - dependence of the SR can be studied by examining Eq. (6-8) in *Chapter 1*. Using $I_e = 100\mu\text{A}$ and $E_e = 11\text{ GeV}$, Eq. (6-8) were numerically integrated (Appendix B.1) between $-1 < \alpha < 1$ and $\Delta\theta = 10\text{ mrad}$, for a uniform magnetic field of $B = 4\text{ T}$ assuming 100% longitudinal polarization.

In Figure 7, the total number of SR and spin light (P_γ) photons radiated is plotted. Also in Figure 7, is a plot the difference between the power of spin light spectra above and below the orbit of the electron

(ΔP_γ). An asymmetry term is defined to be $A = \frac{\Delta P_\gamma}{P_\gamma}$, which was used to nail down the range of energies of the photons which must be measured. Lastly, a plot of sampling time required ($T_s = \frac{\Delta A}{A} = \frac{1}{A\sqrt{2PE_e}}$) to achieve the design precision goals.

It immediately becomes clear that the ionization chamber, which is envisioned to measure the asymmetry (that in turn will be used to compute the electron polarization), will have to be operational at wavelengths corresponding to hard - XRays. Furthermore, the asymmetry plot, Figure 7.D, demands that the sampling be done at the higher energies (and not close to 0.5MeV) since at higher energies the asymmetry is not rapidly changing, thus making it an ideal high-energy polarimetry technique. It might be important to note that the asymmetry is fairly low but since the integrated power of spin-light is very high, the time required for achieving 1% polarimetry is only of the order of a few seconds. Also, one could plot the asymmetry and SR spectra for different energies to study the trends with change in beam energy. This indicates that there are no suppression effects at higher energies that might hinder effective polarimetry.

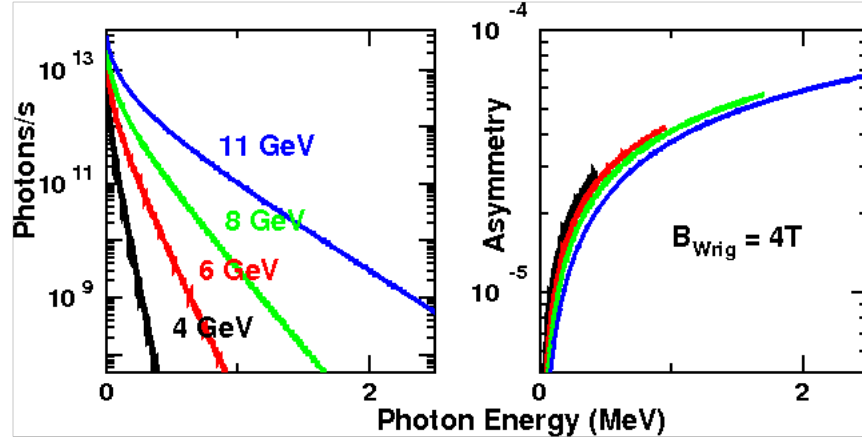


Figure 8: (Left) A. Plot of spin light spectra over photon energies for various electron beam energies ranging from 4GeV – 12GeV; (Right) B. Plot of asymmetry over photon energies for various electron beam energies ranging from 4GeV – 12GeV

3.2 WIGGLER MAGNET

In order to establish the dimensions of the dipoles, the same graphs as in Section 3.1 Figure 8 were plotted for various pole lengths and magnetic fields. First, the asymmetry increases very slowly with field strength as shown in Figure 9, and the figure of merit (time for 1% statistics) improves very slowly with magnetic fields above 3T as shown in Figure 10B, therefore $B = 4\text{T}$ was chosen since 4T wiggler magnets are easily available at light sources around the world. Secondly, an appropriate pole length of $L_p = 10\text{cm}$ was selected by

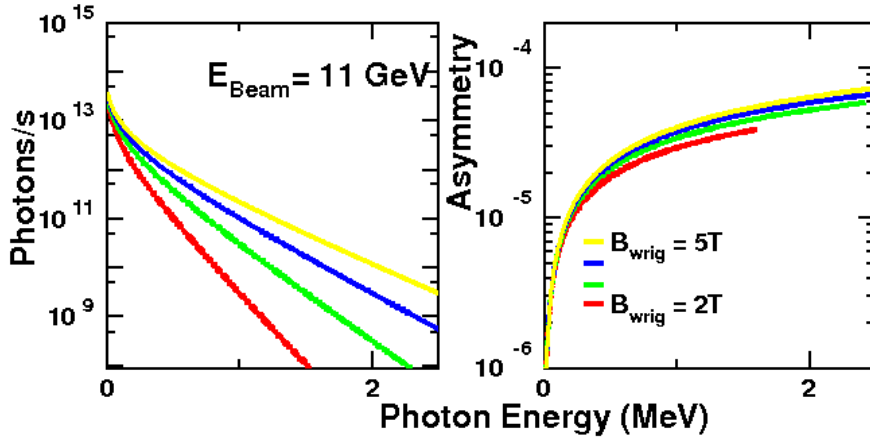


Figure 9: (Left - Right)
 A. Plot of total number of spin light photons P_γ vs. their energy for various pole strengths
 B. Plot of the newly defined term - Asymmetry vs. the photon energies for various pole strengths

looking at Figure 10 and selecting out the pole length for the pole strength of 4Tesla. It is noteworthy to see that the plot of pole length as a function of pole strength was done keeping in mind an SR fan - angular spread of about 10mrad. The plot in Figure 10.B also reassures the reasonable time requirement to achieve the design precision goal of 1%. The last parameter in the wiggler to be fixed is the distance between each dipole.

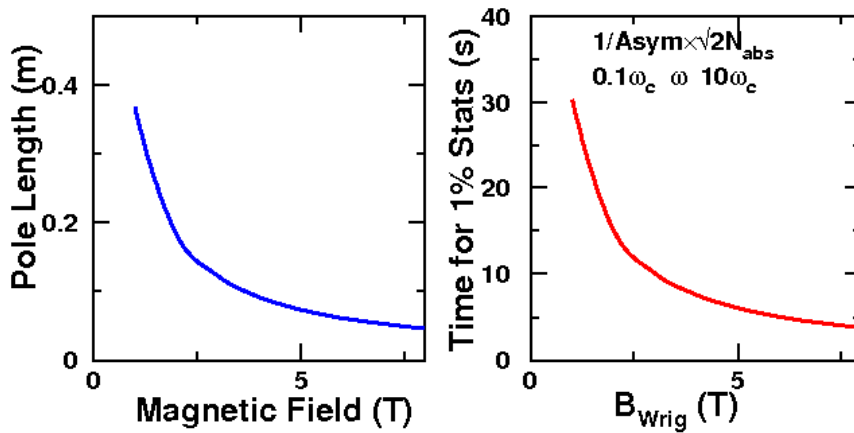


Figure 10: (Left - Right)
 A. Pole length required for a 10mrad angular spread of SR light fans with $B = 4\text{T}$
 B. Dependence of time required to achieve 1% statistics by sampling one wavelength of the spin-light spectra with pole strengths.

3.2.1 Effects of wiggler on the beam

^[16] B. Norum,
CEBAF Technical
note, TN-0019
(1985).

^[17] M. Sands,
SLAC Technical
note, SLAC-121
(1970).

A polarimeter must be non - invasive and therefore answering the question of what would be the effects of putting such as polarimeter on a beam line is very important. But the effect of a high energy electron beam emitting SR has been well studied ^[16]. The number of photons (N) emitted by an electron when it is deviated by a radian, from its initial linear trajectory, when acted upon by a magnetic field is distributed as per the conventional Poisson distribution ^[17] about a mean value of n;

$$\bar{N}(n) = \frac{n^N e^{-n}}{N!} \quad (9)$$

$$n(E_e) = \frac{5}{2\sqrt{3}} \frac{\gamma}{137} = 20.6E_e \quad (10)$$

The average energy of the SR photons can also be written down as {where E_e is the electron energy};

$$\bar{E}_e = \hbar\bar{\omega} = \frac{3 \hbar c \gamma^3}{2 R} = \frac{3 \hbar E_e^3}{2 R m_e^3 c^5} \quad (11)$$

In the case of a spin-light polarimeter, the beam energy is about 11GeV and we choose pole strength to be about 4T in Section 3.2. An angular bend of about 10mrad of the beam is sufficient for such a polarimeter. Using the values of average number of photons emitted and their average energy, the average energy fluctuation ($\Delta\bar{E}_e$) of the beam can be computed.

$$n = 20.62 \times 11_{\text{GeV}} \times .01_{\text{rad}} = 2.06 \quad (12)$$

$$\bar{E}_e = \frac{3 \hbar (11_{\text{GeV}})^3}{2 \cdot 10_m m_e c^5} = .199\text{MeV} \quad (13)$$

$$\frac{\Delta\bar{E}_e}{\bar{E}_e} = \frac{\sqrt{n}\bar{E}_e}{\bar{E}_e} \approx 2.5 \times 10^{-5} \quad (14)$$

The energy fluctuations are smaller than the typical precision with which the energy can be measured at an electron accelerator.

Another parameter which needs to be checked before proceeding, is the transverse kicks ($\Delta\theta_e$) received by the electrons when emitting SR photons in the magnets. The transverse kicks can be calculated in terms of angles knowing that the SR power spectrum usually peaks at an angle $\theta_\gamma = \frac{1}{\gamma}$ ^[17] {where E_γ is the SR - photon energy};

$$\Delta\theta_e = \frac{E_\gamma \text{Sin}(\theta_\gamma)}{E_e} \approx 11.3 \times 10^{-9} \frac{E_{e(\text{GeV})}}{R(\text{m})} \quad (15)$$

$$\bar{\theta}_e = \sqrt{n}\Delta\theta_e \approx 1.5 \times 10^{-8} \text{ (rad)} \quad (16)$$

It can be clearly seen from Eq. (14) and Eq. (16) that both energy fluctuation and angular kicks shall be negligible. This can be seen for all practical purposes in the GEANT-4 simulation that this work demands. This polarimetry method remains a non-invasive procedure.

3.2.2 Effects of realistic dipole magnetic field with fringes

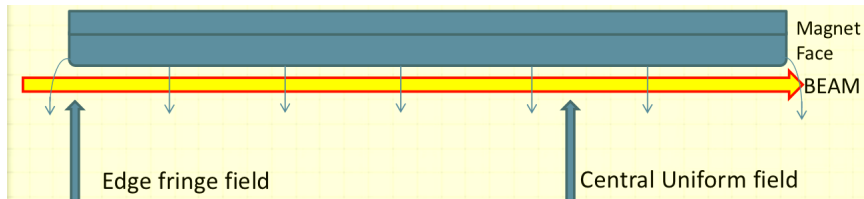


Figure 11: Schematic diagram of the planes at which position the simulation was carried out.

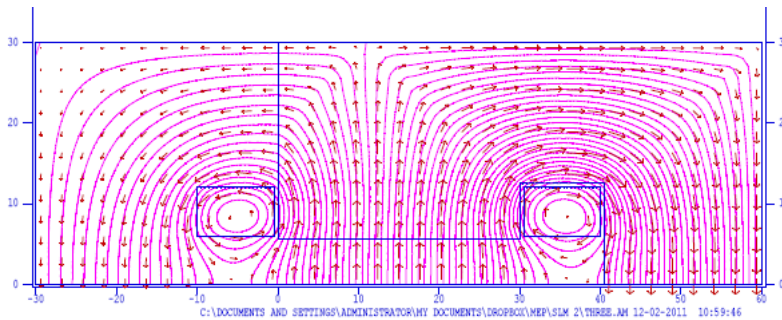


Figure 12: Field map of the dipole face at the center of the dipole.

In Section 3.2, while plotting the power spectra and the asymmetry generated by the code in Appendix B.1 a uniform field was used. But the code can also take a field map. A field map can be generated by solving Maxwell's equations with appropriate boundary conditions. This is essential since field in the transverse plane (perpendicular to the motion of electrons) might distort the SR spectrum and thereby change the asymmetry. In fact there is a custom built suite of programs written by Los Alamos National Laboratory to precisely do this called **LANL Poisson SuperFish** [18].

In LANL SuperFish, the magnet geometry can be easily defined as is done in Appendix B.2. The field map of the magnet can then be plotted. Here, the field map at the edge where the electron beam enters the magnet and at the center of the dipole is presented. In Figures 11 & 13, note that the beam pipe is going at the center below the magnet pole. In Figure 13, the physical taper of the cores can be

[18] Poisson
SuperFish 2D EM
Solver, laacg1.lanl.gov/laacg/services/sfu_04_04_03.phtml, 2007.

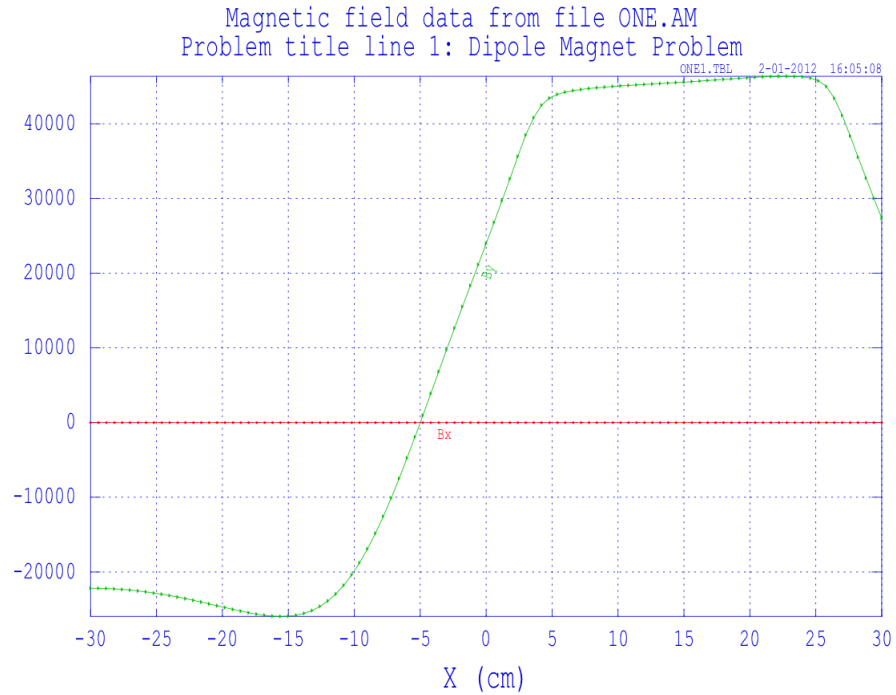


Figure 13: Plot of both the x and y components of the magnetic field on the transverse plane at the center of the dipole (Beam pipe is centered around 15cm mark along the ' x ' axis).

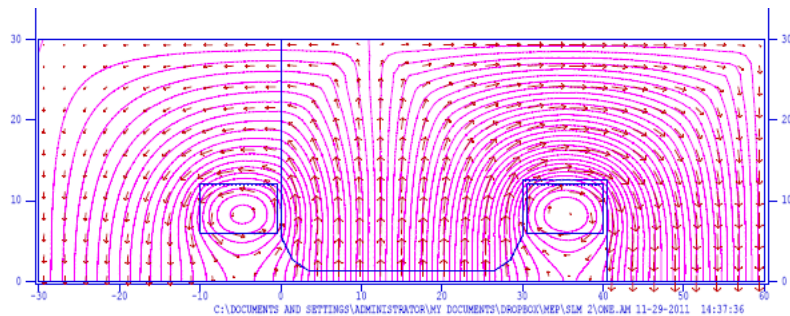


Figure 14: Field map of the dipole face at the edge of the dipole.

notices, since it is at the edge of the magnet face. This taper of the poles is absent in Figure 11, since it is at the center. In Figures 11 & 13, the singularities seen are the areas where the current cuts the plane. Also, it is important to note that the entire 'C' magnet is not visible in the field-map, only the top half of the C magnet is shown in the field map.

X - Axis is to the right and left of the beam and Y - Axis is to the above and below the beam. Also the XY plane is perpendicular to the direction of motion of electron. In Figure 13, it might be important to note that there is no component of the magnetic field. This is because it is at the center of the dipole and there is no fringing of the field. But in Figure 15, there is a non - zero X component to the magnetic field

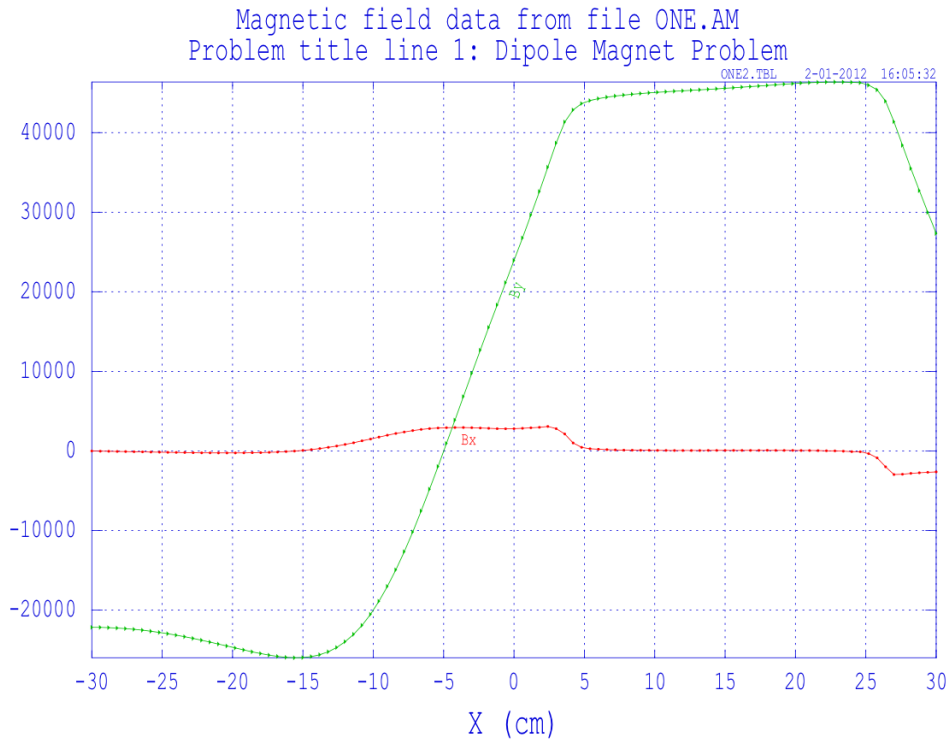


Figure 15: Plot of both the x and y components of the magnetic field on the transverse plane at the the edge of the dipole (Beam pipe is centered around 15cm mark along the 'x' axis).

since it is on the plane at the face of the magnet. A 2D simulation is sufficient since any components along the motion of electrons (Z Axis) will not affect the electrons.

The field map obtained here can be inserted into the numerical integration code (in *Appendix B.1*) and the power spectra and the asymmetry can be obtained. Even though there is a reduction in the total power output of light by introducing a realistic taper for dipole fields, the asymmetry has not changed. This implies that the changes introduced by the realistic dipoles are minimal.

3.3 COLLIMATION AND SPIN-LIGHT FAN SIZE

Even though the distance between the 3 dipoles should in theory not affect the physics involved, it is nevertheless an essential design parameter. A reasonable value of about 1m distance between each dipole was used to start with but this value will be definitely fixed with a full fledged GEANT-4 simulation. A fan with 10mrad spread would then give rise to a spot which is 10cm big in the horizontal plane, 10m from the wiggler where the ionization chambers will be placed. A more important dimension of the SR-spot at the ionization chamber is its height in the vertical direction. An angular spread of

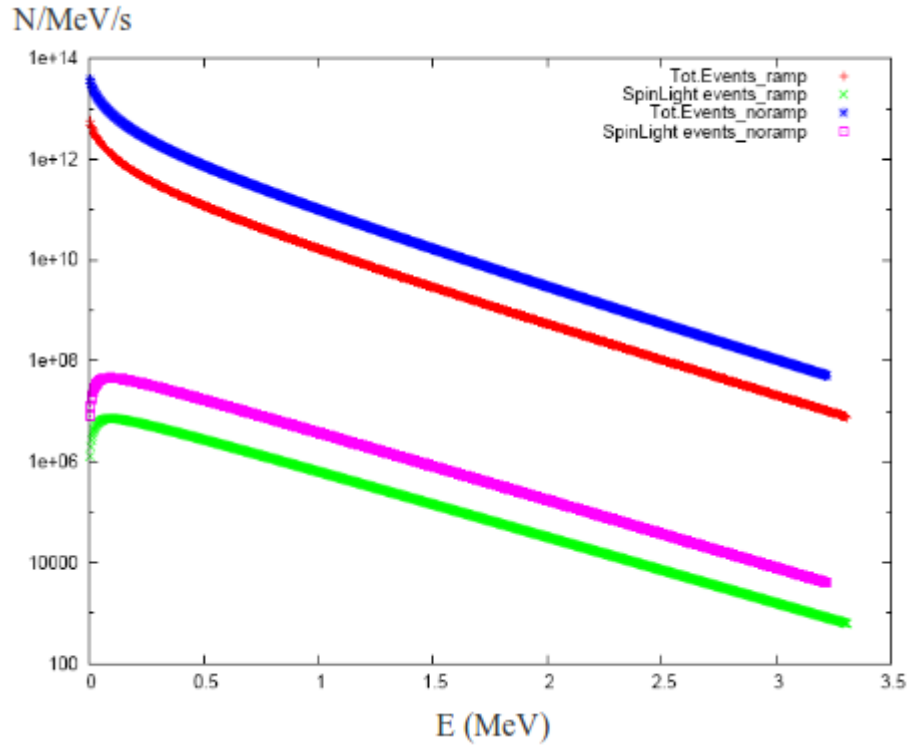


Figure 16: Plot showing the SR - Light (*TotEvents_ramp*) and Spin - Light (*SpinLightEvents_ramp*) power spectra with a realistic taper for the dipoles (Power spectra for uniform magnetic field have also been presented as *_noramp*).

$\Delta\theta = 1/\gamma = 100\mu\text{rad}$ would then give rise to a spot which is 1 mm big in the horizontal plane, 10m from the wiggler, where the ionization chambers will be placed.

Figure 18 shows the origin of 4 different fans of SR Light (which contain the spin-light component) that are being created at the wiggler magnet. Corresponding fans of SR light create 4 spots at the ionization chamber which is located 10m from the wiggler magnet system. The spots at the ionization chamber as shown in Figure 19, merge with each other and may destroy the spacial asymmetry that contains the polarization information. Therefore collimators may be employed at the face of every dipole to select out a small section of the bigger SR fan as illustrated in Figure 20. After collimation the spots are all uniquely separated and 4 distinct spots can be observed at the ionization chamber (as in Figure 21).

3.4 IONIZATION CHAMBERS

The Spin Light polarimeter detector would consist of a position sensitive ionization chamber to measure the up-down asymmetry in the SR - Light. Such a position sensitive detector that could characterize

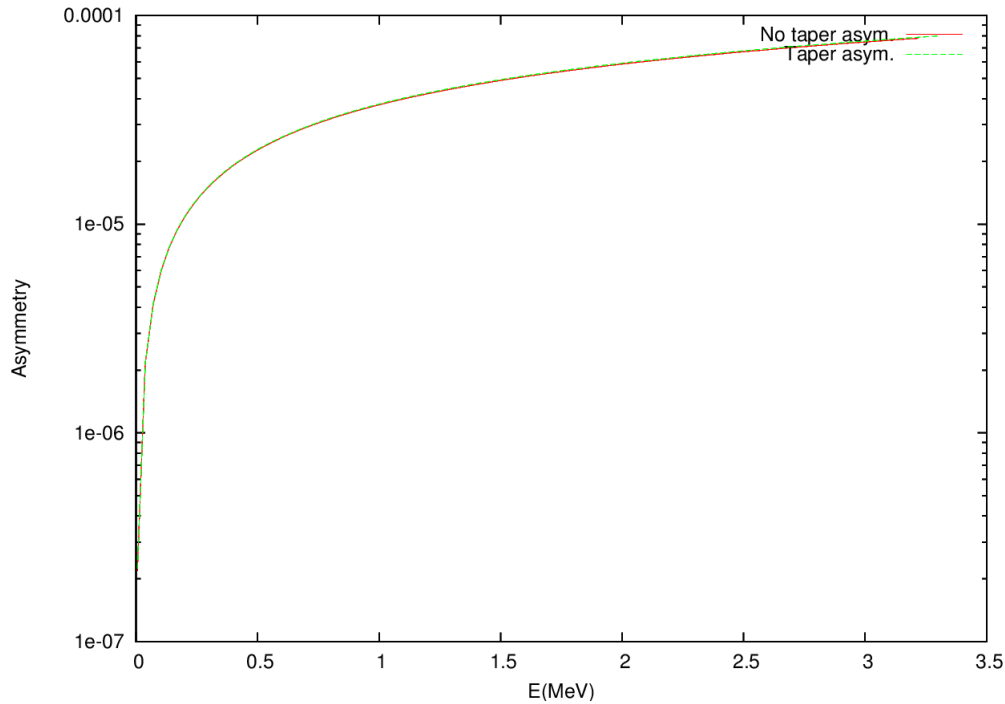


Figure 17: Plot of the asymmetry with a realistic taper for the dipoles (*Taper asym.*).

X-Ray spectrum has already been developed at the *Advanced Light Source*, Argonne National Laboratory and at *Sprin-8 Light Source*. This uses a split - plane which essentially divides the ionization chamber into 2 separate chambers but with a common electrode. These have been demonstrated to have a resolution of about $5\mu\text{m}$ ^[19]. Subtracting the currents from the top chamber from the bottom chamber will then give a measure of the asymmetry in the SR-Light. A schematic diagram of the prototype is presented in Figure 23.

Using such an ionization chamber, one could easily carry out relative polarimetry. A more challenging but possible option would be to have an absolute polarimeter.

3.4.1 Relative Polarimetry

A Xenon media split plate would be an ideal differential ionization chamber. Using Ti windows of sufficient size could in principle cut down on low energy X-Rays ($< 50\text{KeV}$) and Ti has been shown to have a high transparency for hard X-Ray ^[20]. A schematic diagram of the ionization chambers for the Spin-Light polarimeter is presented in Figure 23. The Spin-Light Polarimeter Ionization chamber shall have 2 compartments into which the 2 collimated fans of SR Light will enter. On each side of the electron beam is one split - plane ionization chamber and therefore all 4 fans of SR - Light, produced at the wiggler magnet, are measured at the 2 ionization chambers. Notice for

[19] K. Sato, *J. of Synchrotron Rad.*, 8, 378 (2001); T. Gog, D. M. Casa and I. Kuzmenko, CMC-CAT technical report.

[20] G. Tepper and J. Losee, *Nucl. Inst. and Meth. A* 356, 339 (1995).

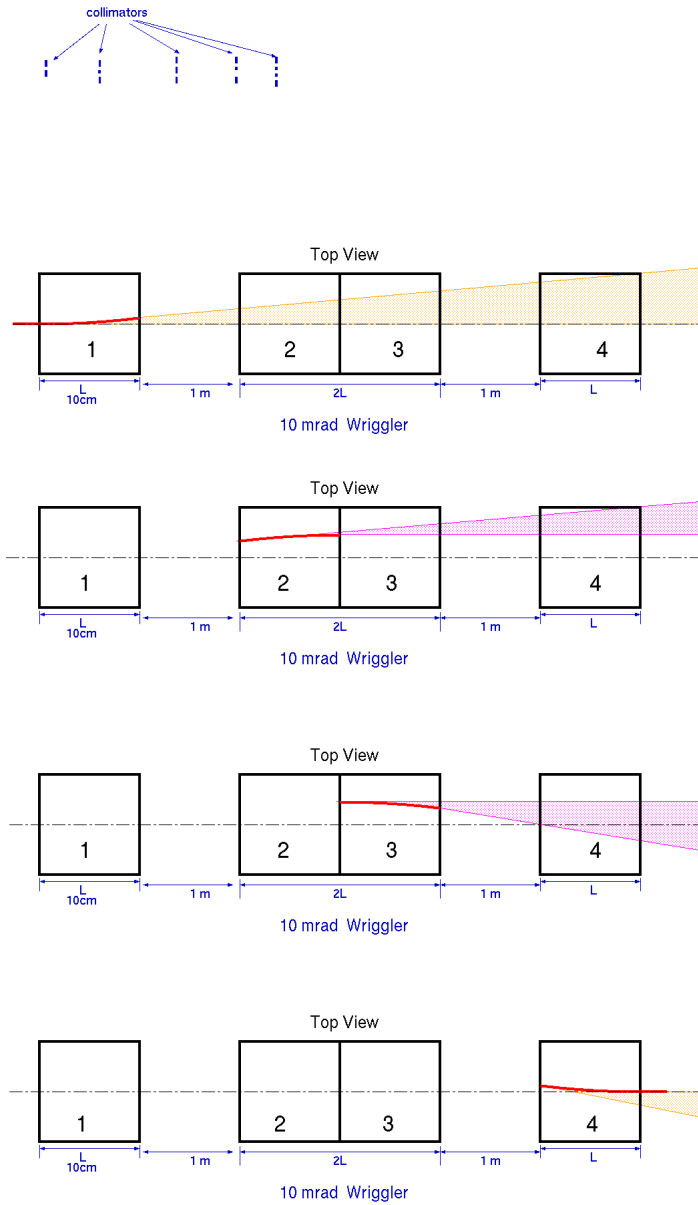


Figure 18: A schematic diagram showing the 4 fans of SR that originate at the wiggler magnet system.

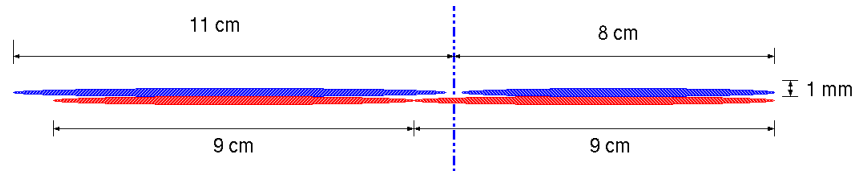


Figure 19: A schematic diagram showing the Spin-Light profile at the Ionization Chamber

polarimetry, just one ionization chamber is required. The 2 separate ICs will provide abundant statistics in a short time.

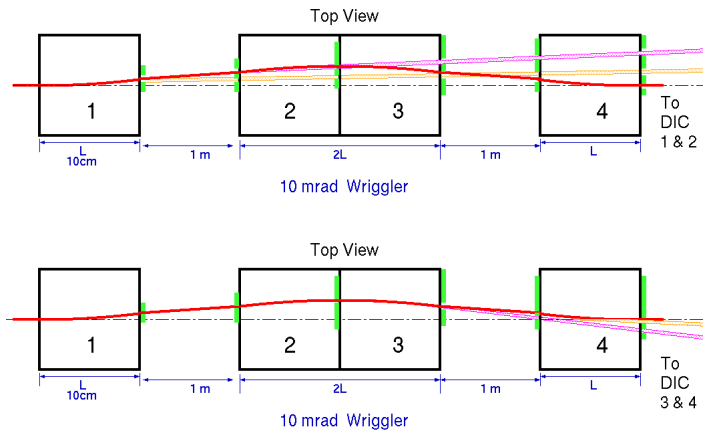


Figure 20: A schematic diagram showing the 4 fans of SR that originate at the wiggler magnet system with collimators.



Figure 21: A schematic diagram showing the Spin-Light profile at the Ionization Chamber with collimators.

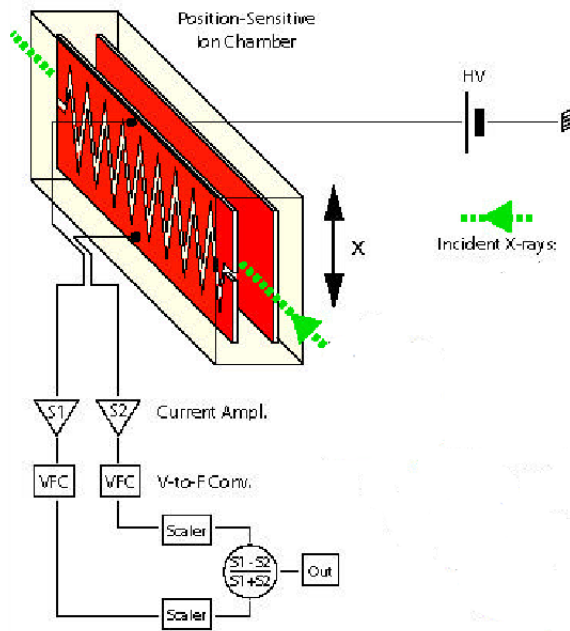


Figure 22: A schematic diagram of a prototype split plate Ionization Chamber.

The signal which will give us a measure of the spacial asymmetry could be measured by subtracting the currents from the UP and DOWN parts of the chamber after being amplified as shown in Figure 24. The spin - light asymmetry shall be of opposite signs on the

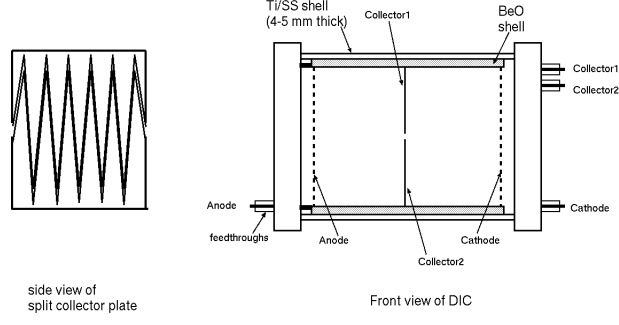


Figure 23: A schematic diagram of the Spin - Light Polarimeter Ionization Chamber.

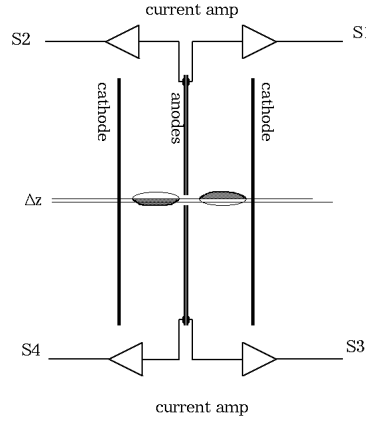


Figure 24: A schematic diagram of signal collection configuration.

LEFT and RIGHT parts of the chamber, since SR fans from adjacent wiggler dipole (which have opposite polarity) enter one on each side of the chamber (L-R). Beam motion effects are nullified as any motion will have have trend (same sign) on both the LEFT and RIGHT sides of the chambers. Each half (T-B) of the split plane collector measures a current proportional to the difference of photon flux between the 2 sides and therefore any vertical beam motion effects cancel out to the first order. The two signals indicated in Figure 24 can be quantified. This definitely shows that the vertical beam motion effects will be canceled out to first order.

$$S_1 = N_{SR}^l + N_{spin}^l + \Delta N_z^l - (N_{SR}^r - N_{spin}^r + \Delta N_z^r) = 2N_{spin} \quad (17)$$

$$S_2 = N_{SR}^l - N_{spin}^l - \Delta N_z^l - (N_{SR}^r + N_{spin}^r - \Delta N_z^r) = -2N_{spin} \quad (18)$$

[21] G. Tepper and J. Losee, *Nucl. Inst. and Meth. A356*, 339 (1995).

{Where $N_{SR}^{l(r)}$ is the number of SR Photons on the left (right) side of the middle split plate, $N_{spin}^{l(r)}$ is the number of spin-light photons and $\Delta N_z^{l(r)}$ is the difference in number of photons introduced by the vertical beam motion}.

Hence $S_1 - S_2 = 4N_{\text{spin}}$ is a measure of longitudinal polarization and $S_1 + S_2$ will give a measure of transverse polarization. The ability to measure both transverse and longitudinal polarization makes this a powerful polarimetry technique. The number of photons absorbed in the ionization chamber can be computed by multiplying the SR Power equation Eq.(8) with the absorption function (where μ is the absorption coefficient which is material specific and t is the length of the chamber) $A(\lambda, t) = 1 - e^{-\mu(\lambda).t}$. With the help of values of μ obtained from NIST database [21], a plot of photons absorbed in a ionization chamber that is 50cm in length and held at 1atm pressure is shown in Figure 25. The spectra of number of photons absorbed was used to then calculate the detector response which in this case is asymmetry weighted against absorption.

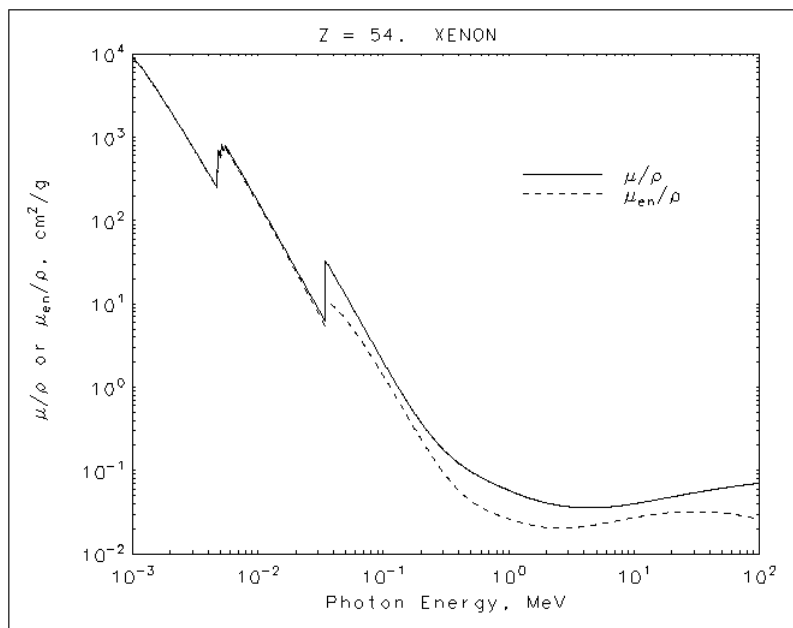


Figure 25: NIST plot of dependence of absorption coefficient of Xenon on the photon energy [21].

3.4.2 Absolute Polarimetry

A relative polarimeter could be turned into an absolute polarimeter by making a few modifications to the ionization chamber. for absolute polarimeter, a high resolution ionization chamber is required and so the natural choice would be a high pressure Xenon IC. A cylindrical chamber capable of withstanding 50atm of pressure could house the IC setup whereas the rest of the structure would remain unchanged from the relative IC with a few additions. The electrodes could be held in place with thin walled BeO ceramic material which would provide uniform electric field and reduce acoustic noise while being transparent to hard XRays [21]. This design eliminates the need for

[22] S. Kubota, M. Suzuki and J. Ruan, *Phys. Rev. B* 21, 2632 (1980).

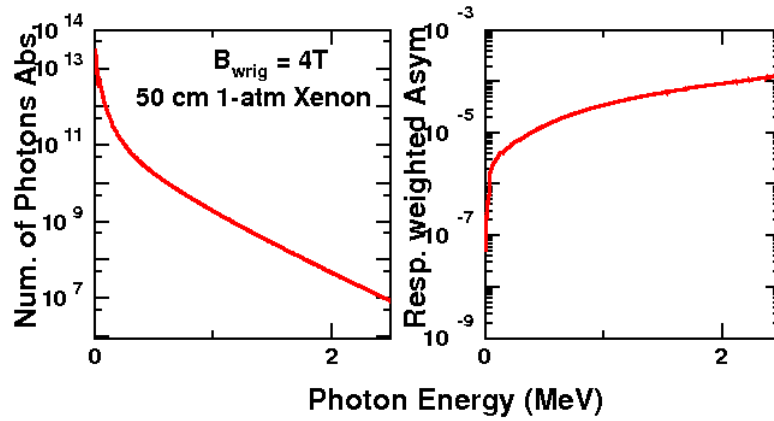


Figure 26: Plot of photons absorption spectra for the ionization chamber.

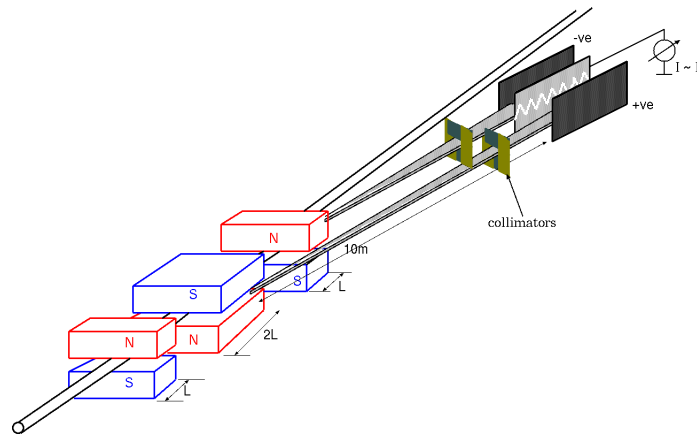


Figure 27: Schematic diagram of the entire Differential Spin Light Polarimeter (The only visible difference between the absolute and relative polarimeters in the schematics is the difference in collector plate bias).

field guide rings which require additional feed throughs and internal voltage dividers. In order to shield against space charge build-up, a wire mesh grid should be placed near the anode which carries a voltage that is intermediate in value to the drift potential (potential between the anode and the cathode). The ratio of the grid field to drift field can be adjusted to maximize the shielding efficiency. The cathodes and the intermediate grids would be build from stainless steel wire mesh to allow the compressed xenon UV scintillation light to be collected by the UV sensitive photomultiplier tubes (PMT). The scintillation signal has a fast component with a decay time of 2.2ns and slow component with a decay time of 27ns^[22]. The scintillation light can be used during calibration, to provide a time zero reference for ionization position determination and can also be used for background suppression using pulse shape discrimination and for anti-coincidence Compton suppression. This will help improve the energy resolution and hence aid the determination of the sensitive en-

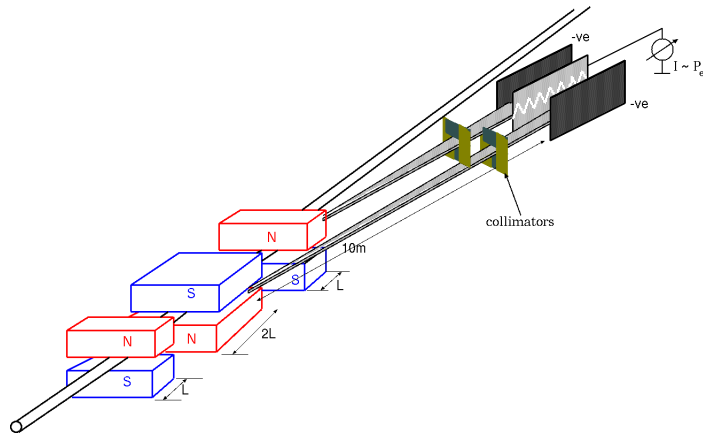


Figure 28: Schematic diagram of the entire Absolute Spin Light Polarimeter (The only visible difference between the absolute and relative polarimeters in the schematics is the difference in collector plate bias).

ergy range of the chamber (during calibration, when the chamber is operated in charge mode). Similar HPXe chamber (without the split anode) have been successfully operated [21] for over a decade now and are also commercially available. A schematic for such an IC is shown in Figure 29. The readout electronics chain would consist of a pre-amplifier and shaping amplifier unlike the current amplifiers used in the current mode ICs. In addition, one would also have to establish the linearity of such an IC given the high flux of photons making the calibration of the IC very challenging. The vertical beam

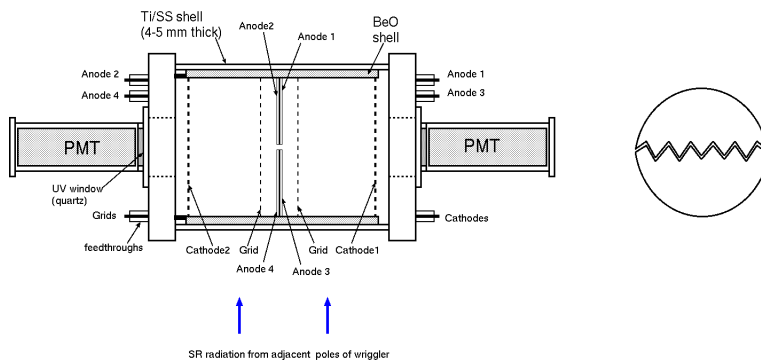


Figure 29: A schematic diagram of the Absolute Spin - Light Polarimeter Ionization Chamber.

motion effects in an absolute IC shall be cancelled to the first order just like in the differential IC. The current signal from each chamber is an integral over the sensitive energy range of the chamber. This energy range convoluted with the detector response function, can be determined by calibrating the chamber at low electron beam currents ($\sim 1\text{nA}$), where the photon flux is low enough to operate the chambers in charge mode. The pulse height spectrum from these calibra-

tion runs can be used to determine the sensitive energy range and the detector response function. The uncertainty in determining the absolute value of the range of energies integrated (specially the lower bound) is the other major source of uncertainty.

In the case of an absolute IC, 4 different signals involving each part (TOP/BOTTOM parts of split plane) and (LEFT/RIGHT) parts of the chamber can be tapped for analysis as shown below.

$$S_1 = I_{SR} + I_{spin} + \Delta I_z \quad (19)$$

$$S_2 = I_{SR} - I_{spin} + \Delta I_z \quad (20)$$

$$S_3 = I_{SR} - I_{spin} - \Delta I_z \quad (21)$$

$$S_4 = I_{SR} + I_{spin} - \Delta I_z \quad (22)$$

{Where I_{SR} is the current due to all SR Photons and I_{spin} is the current due to just the spin- light photons}.

The signal $(S_1 + S_2) - (S_3 + S_4)$ should always be zero ideally. The longitudinal asymmetry in terms of these 4 signals is given by;

$$A^{long} = \frac{I_{spin}^{long}}{I_{SR}^{long}} = \frac{(S_1 - S_2) - (S_3 + S_4)}{(S_1 + S_2) + (S_3 + S_4)} \quad (23)$$

and the transverse asymmetry in terms of these 4 signals is given by;

$$A^{trans} = \frac{I_{spin}^{trans}}{I_{SR}^{trans}} = \frac{(S_1 + S_3) - (S_2 + S_4)}{(S_1 + S_3) + (S_2 + S_4)} \quad (24)$$

One could in theory come up with many more electrode arrangements.

3.4.3 Effects of Extended Beam Size

In *Section 3.2*, the numerical code used a point beam. Therefore the effects of having extended beam size of about $100\mu\text{m}$ must be studied. To do this the code located in *Appendix B.3* was used. This code essentially superimposes the SR-Power spectra generated by each of a 10^6 such point-cross section beams. The million point - cross section beams together would give a circular beam and each of them was weighted with a Gaussian profile in order to make the extended beam a perfect Gaussian beam. The cumulative spectra can be plotted

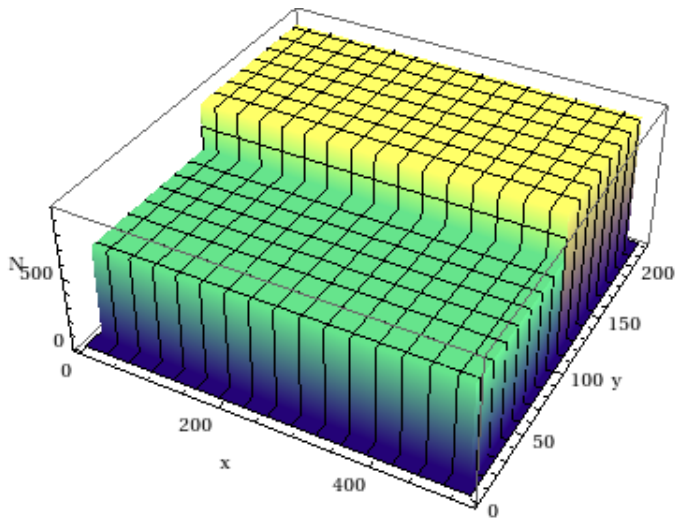


Figure 30: Integrated power spectra of SR Light at the IC due to a point-cross section beam - $X, Y(10\mu\text{m})$; $N(\times 10^{12})$. (The difference between the profile has been enlarged for clarity)

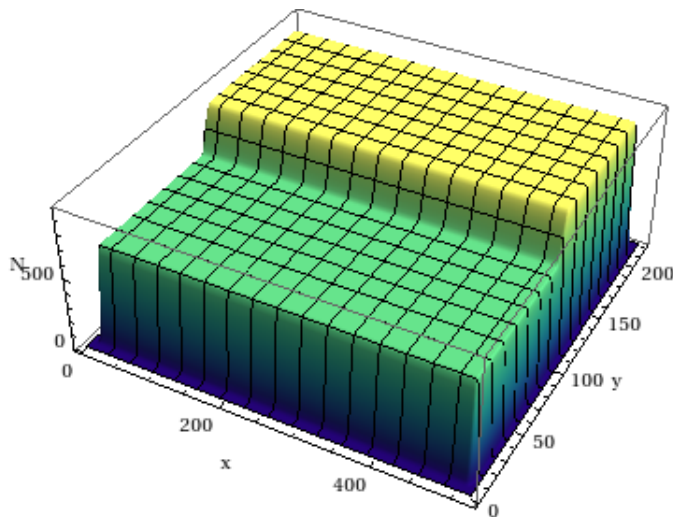


Figure 31: Integrated power spectra of SR Light at the IC due to a real beam of size ($R_{\text{beam}} = 100\mu\text{m}$) - $X, Y(10\mu\text{m})$; $N(\times 10^{12})$. (The difference between the profile has been enlarged for clarity)

and one can guess that it should have the same structure as the original spectra for the point - cross section beam. This is so because the size of the beam ($R_{\text{beam}} = 100\mu\text{m}$) is small compared to the size of the collimated SR - Light spot which is about 1 mm big. For the beam with a point cross section, the SR - profile is rather 'box' like at the IC. When an extended beam, that is Gaussian profile, is introduced, the SR - profile gets a taper which is Gaussian in nature too. The graphs in Figure 30 and 31 show the exact 3D profile correct with position information.

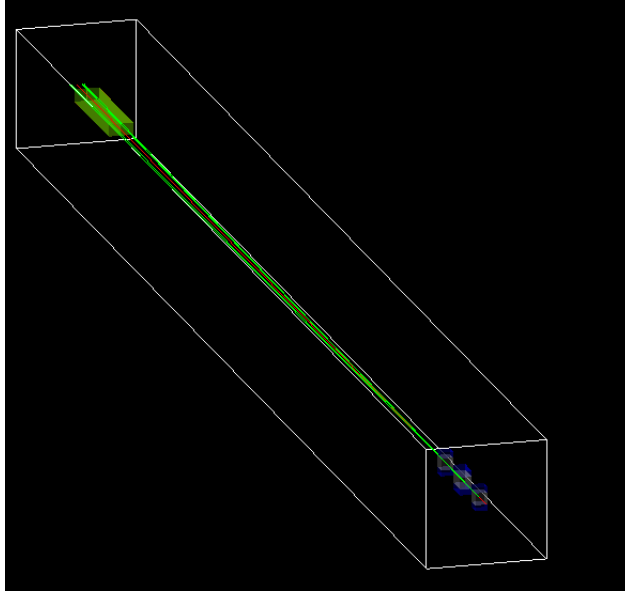


Figure 32: GEANT₄ visualization of Spin - Light Polarimeter Setup. The electron beam is red in color and the SR Fans are yellow in color.

Geant₄ has been a widely used tool-kit to simulate interactions of particle beams with matter and fields. Originally developed at CERN in Geneva, Switzerland, its development has been decentralized over the last decade. Geant₄ does include synchrotron radiation (SR) physics under the standard electromagnetic physics list.

Geant₄ SR process has been rigorously validated at Stanford Linear Accelerator Center in Palo Alto, CA and at Fermi National Accelerator Laboratory in Batavia, IL ^[23],^[24]. It might be important to note that this validation of the SR process is only valid if the beam is made up of electrons in few GeV energy range with SR photon energy spectra peaking at energies much lower than the energy of the beam which means that the electrons passed through magnets with a few tesla field. That is, the Geant₄ SR process might not work if the magnets have magnetic fields close to the B_c which is upwards of 100T. Since the magnetic field in this Spin-Light Polarimeter is near about 4T, and from Figure 7 (in Chapter 3) it can be seen that an 11GeV electron beam (which is one of the proposed electron beam injection energies in both the EIC designs of eRHIC and ELIC), the SR photon energy spectra peaks near about few MeV and therefore using Geant₄ to simulate SR photons is justified. This work demands a Geant₄ simulation in order to optimize the distance between the dipoles and to

^[23] F. Herlach, R. McBroom, T. Erber, J. Murray, and R. Gearhart: *Experiments with Megagauss targets at SLAC*, IEEE Trans Nucl Sci, NS 18, 3 (1971) 809-814.

^[24] T. Erber, G. B. Baumgartner, D. White, and H. G. Latal: *Megagauss Bremsstrahlung and Radiation Reaction*, Proceedings of High Energy Accelerators (1983), 372-374.

optimize the positioning of the collimators. Figure 32 is a Geant4 visualization of the entire setup. It is important to note that the 2 fans are clearly visible on either side of the beam in the center.

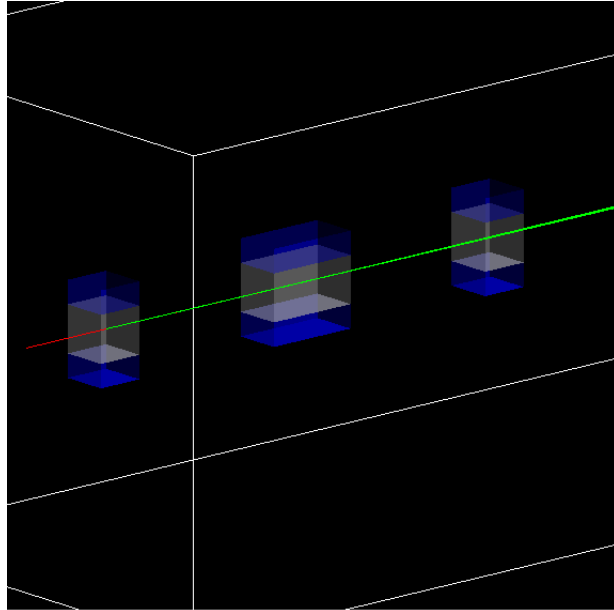


Figure 33: GEANT4 visualization of Wiggler Magnet Setup.

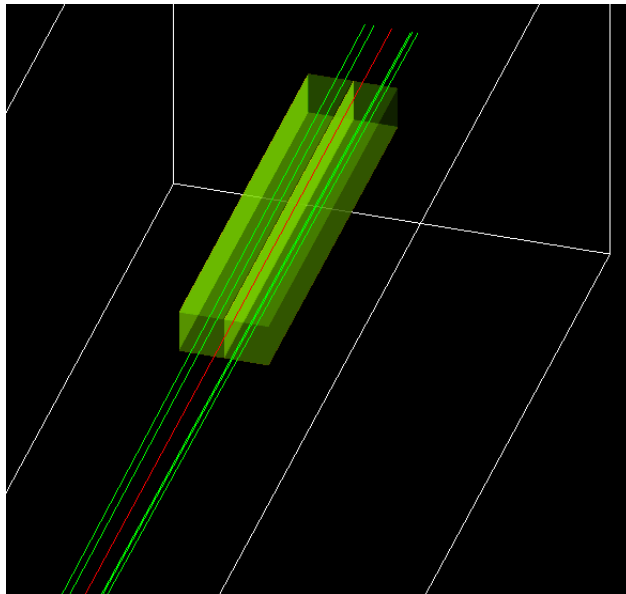


Figure 34: GEANT4 visualization of the 2 Ionization Chamber Setups (One on either side of the beam).

The entire geometry of the setup including the 3 wiggler magnets, 2 ionization chambers and, the 5 collimators were coded into the Geant4. The geometry construction file is available as an appendix (*Appendix B.4*). A visual rendering can be seen in Figure 32. As demonstrated in *Chapter 3*, Figure 19, the collimators select 4 (2 on each side

of the electron beam) unique slivers of the bigger SR fan. This can be clearly seen in Figure 34.

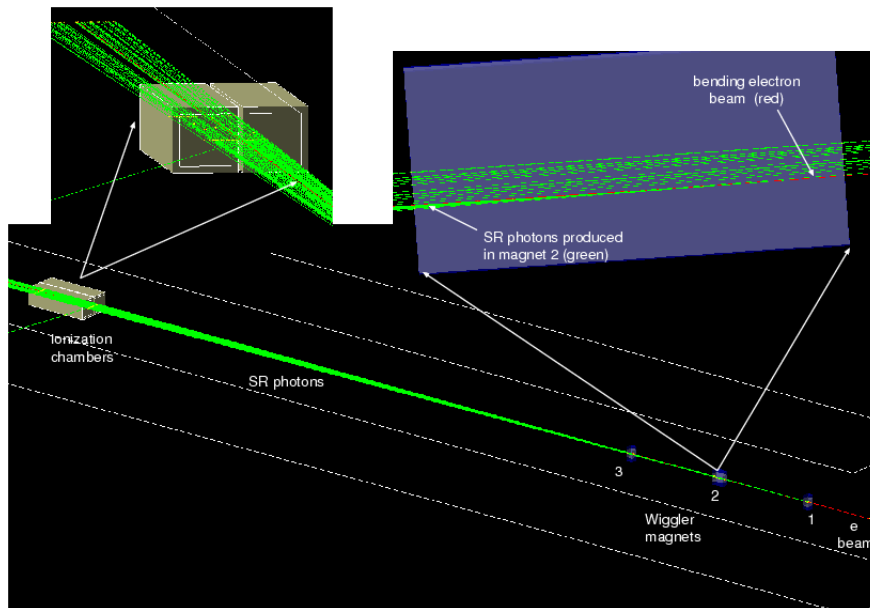


Figure 35: SR fans produced by a few 11 GeV electrons.

It might be fun to spot the electron beam bending in the magnetic field as shown in Figure 35. The code was tested with a few electrons for a 11GeV beam. Some simple observations that could be made straight away without measuring anything would be;

- The electron beam returns to its original linear trajectory (as along the initial electron gun firing vector). This means that the magnets are aptly separated with appropriate fields.
- The red colored electrons produce yellow colored photons in conical fans.

4.1 SPIN LIGHT IN GEANT4 AND ASYMMETRY

Even though the integrated energy spectrum (over all angles which includes above and below the electron orbit in the wiggler magnets) is validated, the angular dependence of SR light is not in Geant4. Therefore one would have to add the angular dependence in Equation 4 (*Chapter 1*) to the Geant4 SR process in the standard electromagnetic list. Alternatively, one could modify their application created using standard Geant4.9.6 source code and add the SR angular dependence into their stacking action. Our Spin-Light simulation application implements the Spin-Light by manipulating the spacial asymmetry according to *Section 3.1*. The asymmetry can be linear polynomial parameterized as:

The complete Spin-Light Geant4 Simulation package can be accessed at spinlight.mohanmurthy.com

$$A(E) = (4.5 \times 10^{-7}) + (5.7 \times 10^{-5}E) - (3.0 \times 10^{-5}E^2) + (1.3 \times 10^{-5}E^3) - (3.3 \times 10^{-6}E^4) + (3.2 \times 10^{-7}E^5) + \Theta(E^6)\dots \quad (25)$$

{ A is the asymmetry and E is the energy of the SR photon}

At the event stacking level, the SR photons are killed with a probability equal to asymmetry calculated by Equation 25. This creates an up-down asymmetry in the SR cones which is vital for successful simulation of a Spin-Light polarimeter.

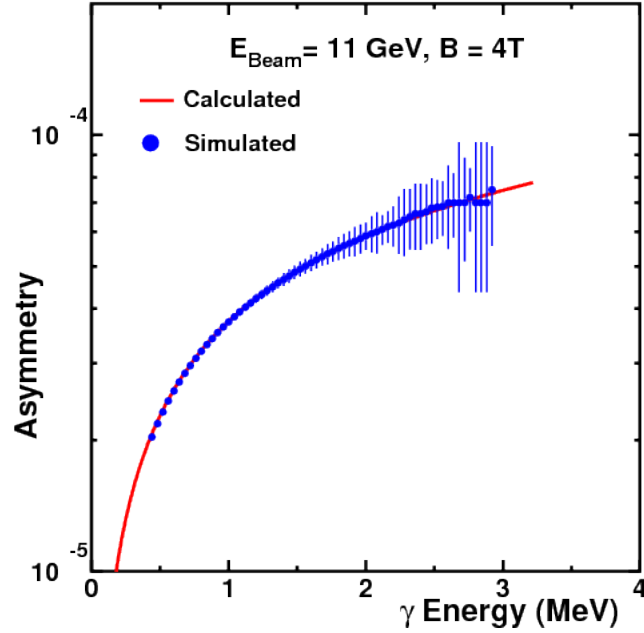


Figure 36: Geant4 Asymmetry compared with physics asymmetry

As seen in Figure 36, the simulated asymmetry closely matches the physics asymmetry curve within 1%. It is important to note that the parameterization shown is only good in relevant range of photon energies (0 – 3.5 GeV). Anyone who would like to use this parameterization beyond this relevant range would have to fall back on the numerical code in *Appendix B.1*.

A histogram of SR photon energies is then constructed. By dividing the difference of number of photons with positive momentum and number of photons with negative momentum with the total number of SR photons, a spin-light spectrum was made as shown in Figure 37. But before plotting the histograms were scaled up since some photon tracks were killed in the stacking action. This should be acceptable as the asymmetry is usually very small and so the scale factor is very close to 1 (~ 1.0001). In Figure 37, the power spectra seems to deviate at low energies (close to about 0.5 GeV. This is the case as the SR photon characteristics plotted in Figure 37 are characteristics of SR

photons as detected at the IC and for this measurement, a 0.3mm solid lead window was used to eliminate low energy X-Rays below 0.5GeV. Eliminating X-Rays below 0.5GeV is particularly important as most of the SR photons are low energy photons, but the asymmetry is low at low energies contributing to very small numbers of spin-light photons. In essence, the low energy photons are junk! Once it is made sure that the energy spectra matches the physics prediction very closely, the corresponding power spectra is easy to calculate and plot as in Figure 38.

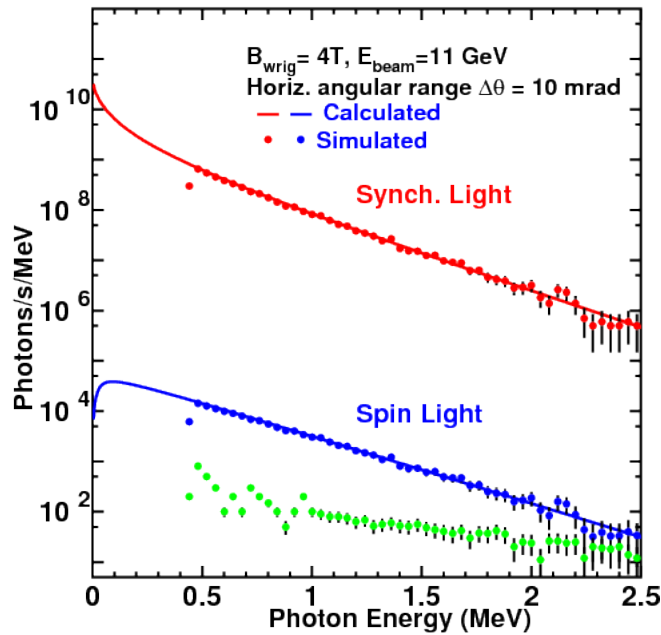


Figure 37: Geant4 SR and SL spectra as compared with physics SR and SL spectra

4.2 SYNCHROTRON LIGHT PROFILE AT THE IONIZATION CHAMBERS AND COLLIMATION

The collimators are vital to separate the fans from each magnet so that the spacial asymmetry is intact as predicted by the simple physics model that was developed in *Chapters 1 & 2*. Without the collimators the SR light profiles would all mix and might not necessarily help linear polarimetry (linear to the polarization of electrons in the beam). Therefore, the 4 slivers selected by 5 collimators must not mix and the ionization events created by these SR photons should be clearly resolvable in space at the ionization chambers. With the collimator opening width of about 100 μ m, the 4 SR slivers are clearly resolved as shown in Figure 39.

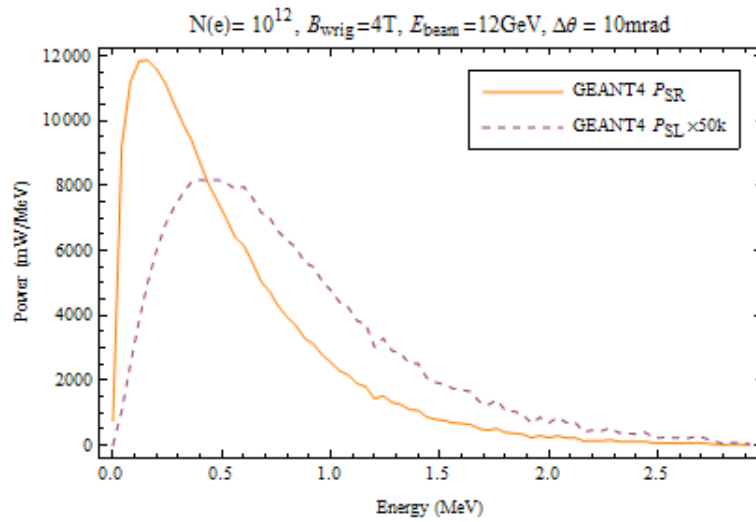


Figure 38: Geant4 SR and SL power spectra

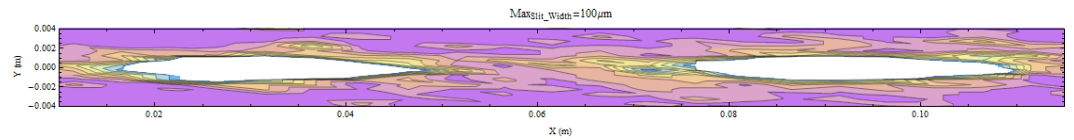


Figure 39: A contour plot of the number of events generated by the 2 slivers of the SR fan in one of the ionization chambers. The white regions are regions of high event density and the blue regions have a low event density.

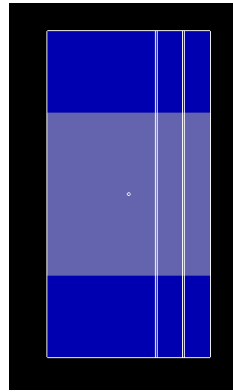


Figure 40: Position of collimators on the face of magnet 2 facing magnet 1.

With the help of Figure 20 (*Section 3.4*), it can be seen that photons in each [of the 2] spot in the Figure 39 comes from a unique dipole magnet (numbered 1 through 4, the central dipole consists of 2 "parts" as it is twice as long as the other two). Even though each spot is only suppose to contain photons from one specific [dipole magnet] part, a source of error is introduced here since this is not always the case. For example consider the IC on the left hand side of the beam which has spots from dipole magnet part # 1 & 2. In this case, the left

hand side spot in Figure 39 should contain photons from dipole magnet part 1 and the right hand side spot must contain photons from dipole magnet part 2. But, some photons from dipole magnet part 1 seep into the spot on the right hand side. If the percentage of these photons is $\sim 0.1\%$ we consider the spots resolved. The size of the collimators is an important factor which determines if these spots are completely resolved. With a collimator slit width of about $100\mu\text{m}$ the spots are completely resolved. Another source of error here could be from bremsstrahlung events from the photons impinging on the collimators. These bremsstrahlung photons contribute to no spin-light events and therefore are junk events. Fortunately these events comprise of about only $\sim 0.1\%$.

SUMMARY

5.1 SYSTEMATICS

If the ionization chambers are used in differential mode and have split anodes, the false asymmetries will cancel to first order. Moreover, since the signal used is a differential signal the size of the background must be small compared to the signal. A full simulation is needed to study the background and the asymmetry associated with the background. In the experiment the background can be determined by monitoring the difference in the signal from the chambers with the wiggler magnets turned on and off. The other major source of systematic uncertainty is the lower bound of the integration window used to generate the IC signals. The absolute value of the spin light asymmetry depends on the absolute value of the energy window over which the IC signals are integrated. It is especially sensitive to the lower bound because of the steep fall of the SR intensity with energy. However given the excellent energy resolution that has been demonstrated for HPXe ionization chambers, one should be able to calibrate the chamber and determine the response function and the lower bound of the chamber to better than 2%. A preliminary table of estimated systematic uncertainties is shown in table below.

Source	Uncertainty	$\delta A/A$
Dark Current	pA	< 0.01%
Intensity Fluctuations	$\Delta N \times 10^{-3}$	< 0.10%
Beam Energy	1.0×	< 0.05%
Density of gas in IC	Relative uncertainties	< 0.05%
Length of Chamber	Can be corrected	-
Band - width of X - Rays	2% (for only absolute polarimetry)	1.20%
Background related Dilutions	To be determined if known to 0.5%	< 0.50%
Other dilutions	Cancel to First Order	< 0.50%
Total	Relative Polarimetry	< 0.68%
	Absolute Polarimetry	< 1.88%

Table 1: Systematic uncertainties

5.2 CONCLUSION AND FUTURE WORK

Spin light based polarimetry was demonstrated over 30 years ago, but has been ignored since then. The figure of merit for such a polarimeter increases with electron beam energy and the strength of magnetic field used. The 11GeV beam at JLab is well suited for testing a spin light polarimetry and such a polarimeter would help achieve the 0.5% polarimetry desired by experiments envisioned for the EIC era. A 3 pole wiggler with a field strength of 4T and a pole length of 10cm would be adequate for such a polarimeter. A dual position sensitive ionization chambers with split anode plates is ideally suited as the X-ray detector for such a polarimeter. The differential detector design would help reduce systematic uncertainties. Locating a reasonable piece of beam-line real estate is however very challenging.

[25] V. N.
Litvinenko, *Gatling
Gun: High Average
Polarized Current
Injector for eRHIC,
EIC BNL
Whitepapers (2012)*

Given that the eRHIC design of EIC involves using a Gatalin gun [25], the recovery time of the spin-light IC will need to be less than a second if every bunch of electron beam is to be measured for polarization. So the next thing to do would be create a survey of all experiments beings proposed and their corresponding polarimetry requirements both in terms of precision of polarimetry required and the rate of measurement. Finally it still remains a challenge to secure ample grants in excess of quarter million dollars over the next few years in order to construct a prototype of a Spin-Light Polarimeter for demonstration purposes. VEPP storage ring in Novosibirsk could be a place to test such a prototype.

LISTS AND PERMISSIONS

A.1 LIST OF FIGURES

Fig.	Sec.	Caption (in short)
i	For.	eRHIC @ Brookhaven National Laboratory.
ii	For.	ELIC @ Jefferson National Accelerator Laboratory.
1	1.1	Angular distribution of synchrotron radiation.
2	1.2	Magnetic snake used at the VEPP-4.
3	1.2	VEPP-4 Polarization Experiment.
4	2.1	3-Pole Wiggler.
5	2.2	4 SR fans created by the wiggler magnets.
6	2.3	Cs ¹³⁷ events in a Xenon IC.
7.	3.1	SR-SL spectra, Asymmetry & Time requirement.
8.	3.1	SL, Asymmetry spectra dependence on dipole field.
9.	3.1	SR, Asymmetry spectra dependence on dipole field.
10.	3.1	Pole Length & Time requirement with dipole field.
11.	3.2	Schematic of half a dipole.
12.	3.2	Field map at the center of a dipole.
13.	3.2	Magnetic field at the center of a dipole.
14.	3.2	Field map at the face of a dipole.
15.	3.2	Magnetic field at the face of a dipole.
16.	3.3	SR, SL spectra with realistic magnetic field.
17.	3.3	Asymmetry with realistic magnetic field.
18.	3.4	Schematic of 4 X SR Fans from wiggler.
19.	3.4	Schematic of the 4 X spots at IC.
20.	3.4	Slivers of IC selected by the Collimator.
21.	3.4	Schematic of 4 X spots after Collimation.
22.	3.4	Schematic of Split plane IC.
23.	3.4	Schematic of Split plane IC, side view.
24.	3.4	IC Signal Collection.
25.	3.4	Xenon Absorption coefficient spectra.
26.	3.4	SR Absorption and Asymmetry spectra.
27.	3.4	Schematic of differential polarimeter.
28.	3.4	Schematic of absolute polarimeter.

29.	3.4	Schematic of Absolute Split plane IC, side view.
30.	3.4	Integrated SR Spectrum at IC with point beam.
31.	3.3	Integrated SR Spectrum at IC with Gaussian beam.
32.	4.0	Geant4 visualization of Spin-Light Polarimeter.
33.	4.0	Geant4 visualization of wiggler magnets.
34.	4.0	Geant4 visualization of ICs.
35.	4.1	Few event visualization in the Polarimeter.
36.	4.1	Geant4 Asymmetry Spectra.
37.	4.1	Geant4 SR-SL Spectra.
38.	4.2	Geant4 SR-SL Power Spectra.
39.	4.2	Collimated SR Spots at IC.
40.	4.2	Collimators on magnet 2 back face.

Table 2: List of Figures

A.2 LIST OF REFERENCED PUBLICATIONS

[#]	Publication
i	eRHIC, www.bnl.gov/cad/eRhic/ , 2011.
ii	ELIC @ CEBAF, casa.jlab.org/research/elic/elic.shtml , 2011.
1	D.Dutta et. al, Proposal to the EIC R & D: spinlight.mohanmurthy.com .
2	D. D. Ivanenko et. al., 16, 370 (1946)
2	J. Schwinger, Phys. Rev. 75, 1912 (1947)
3	I. M. Ternov et. al., Univ. Ser. Fiz. Astr. 24, 69 (1983)
3	V. A. Bordovitsyn et. al., Nucl. Inst. and Meth. B266, 3708 (2008)
4	A. A. Sokolov et. al., JETF 23, 632 (1952).
5	A. A. Sokolov et. al., Rad. from Rel. e^- , A.I.P. Transl. Sr. (1986).
5	I. M. Ternov, Physics - Uspekhi 38, 409 (1995).
5	S. A. Belomestnykh et al., Nucl. Inst. and Meth. 227, 173 (1984).
6	K. Sato, J. of Synchrotron Rad., 8, 378 (2001).
7	J. Le Duff et. al., Rapport Technique, 4-73 (1973).
8	A. E. Bolotnikov et. al., Nucl. Inst. and Meth. A396, 360 (1997).
9	T. Doke, Portugal Phys. 12, 9 (1981).
10	V. V. Dmitrenko et al., Sov. Phys.-tech. Phys. 28, 1440 (1983).
10	A. E. Bolotnikov et al., Sov. Phys.-Tech. Phys. 33, 449 (1988).
11	C. Levin et al., Nucl. Inst. and Meth. A332, 206 (1993).
12	G. Tepper et. al., Nucl. Inst. and Meth. A356, 339 (1995).

13	A. E. Bolotnikov et. al., Nucl. Inst. and Meth. A383, 619 (1996).
14	G. Tepper et. al., Nucl. Inst. and Meth. A368, 862 (1996).
15	Proportional Technologies Inc., www.proportionaltech.com .
16	B. Norum, CEBAF Technical note, TN-0019 (1985).
17	M. Sands, SLAC Technical note, SLAC-121 (1970).
18	EM Solver, laacg1.lanl.gov/laacg/services/sfu_04_04_03.phtml , 2007.
19	K. Sato, J. of Synchrotron Rad., 8, 378 (2001).
19	T. Gog et. al., CMC-CAT technical report.
20	G. Tepper and J. Losee, Nucl. Inst. and Meth. A356, 339 (1995).
21	G. Tepper and J. Losee, Nucl. Inst. and Meth. A356, 339 (1995).
22	S. Kubota, M. Suzuki and J. Ruan, Phys. Rev. B 21, 2632 (1980).
23	F. Herlach et. al., IEEE Trans Nucl Sci, NS 18, 3 (1971) 809-814.
24	T. Erber et. al., Proc. of High Energy Accelerators (1983), 372-374.
25	V. N. Litvinenko, Gatling Gun for eRHIC BNL Whitepapers (2012).

Table 3: List of Reference Publications

A.3 LICENSE

GNU GENERAL PUBLIC LICENSE: All the programs are free software; you can redistribute it and/or modify it under the terms of the GNU General Public License as published by the Free Software Foundation; either version 2 of the License, or (at your option) any later version.

This program is distributed in the hope that it will be useful, but *without any warranty*; without even the implied warranty of *merchantability* or *fitness for a particular purpose*. See the GNU General Public License for more details.

ESSENTIAL CODES

B.1 NUMERICAL INTEGRATION OF THE SR - POWER LAW

Listing 1: Fortran 77 Code

```

1 C
C   PROGRAM Ngamma.f (WRITTEN BY D. Dutta 1/7/2010)
C   and
C   Ngammaspectra.f by Prajwal Mohanmurthy (Sept 2011),
C   prajwal@jlab.org, Mississippi State University
6 C
C   To include effects from the Real Magnetic field
C   with non-zero gradient taper.
C
C   This program calculates the total number (and
11 C   difference in number above and below the orbital
C   plane) of Synchrotron photons emitted by longitudinally
C   polarized electrons over a horizontal angular range of
C   dTheta and verticle angular range of;
C
C           +/-alpha = +/-gamma*Psi
16 C   where gamma is the Lorentz boost, i.e.;
C           +/-alpha approx = +/-1
C   when traversing a 3 pole wiggler magnet with a field
C   stength of Bwg tesla and a pole length of Lwg.
C
21 C   IMPLICIT DOUBLE PRECISION (A-H,O-Z)
C
C   IMPLICIT real*8(A-H,O-Z)
C   external fn01
C   external fn02
26 C   external gn01
C   external gn02
C   real*8 xheeng(48),xhemu(48),couB(15)
C   real*8 couxn,coudn
C
31 C   parameter (xMe=0.510998902) !electron mass in MeV/c^2
C   parameter (GeV2MeV=1000.0)
C   parameter (hbarc=197.3269602) ! MeV*fm
C   parameter (xmuB=5.788381749E-11) ! Bohr magnetron MeV/T
C   parameter (c=299792458) ! m/s
36 C   parameter (pi=3.141592654)
C   parameter (qe=1.602176462E-19) ! coulomb
C   parameter (n1=10) ! number of times the integration alg is
C           compounded
C   parameter (n2=10)

```

```

41      Common gamma,y
      C      write(6,*)'Enter Ebeam (GeV) and current (micro A)'
      C      read(5,*)Ebeam,xIe
      C      write(6,*)'Wiggler B-field (T) and Pole length (m)'
46      C      read(5,*)Bwg,xLwg
      do i = 1,15
          couB(i)=4.55
      enddo
      couB(1)=4.11
51      couB(2)=4.38
      couB(14)=4.38
      couB(15)=4.11
      open(unit=10,file="spinlight_gydep4.dat",status="unknown")
      open(unit=11,file="xenon.dat",status="old")
56      do i =1,48
          read(11,*)xheeng(i),xhemu(i)
      enddo
      close(11)
      ymin = 0.01 ! min fractional photon freq (W/Wc)
61      ymax=0.02 !initialize
      C      Ebeam=4.0+(i-1)*1.0 ! e-beam energy GeV
      Ebeam=11.0 ! e-beam energy GeV
      xIe=100.0 ! e-beam current micro A
      do i=1,1000
66      do j=1,15
          couxn=0.0
          coudn=0.0
          Bwg=couB(j) ! B-field in T
      C      Bwg=1.0+(i-1)*1.0
71      C      xLwg=0.066 ! pole length in m
      C      write(6,*)'Ebeam =',Ebeam, 'GeV'
          gamma = Ebeam*GeV2MeV/xMe ! Lorentz boost = E/(Me*c^2)
          R_bend = gamma*hbarc*1.0E-15/(2.*xmuB*Bwg) !bending
              radius in m
          Omega_o = c/R_bend ! betatron freq.
76      Omega_c = 1.5*gamma**3*Omega_o ! central photon
              frequency
          E_cent=(Omega_c*hbarc*1.0E-15/c)*1000. ! central photon
              energy in keV
          xlambda_c=2.*pi*c/Omega_c
          ymax = 0.02+(i-1)*0.01 ! max fractional photon freq (W/
              Wc)
          y_cent= (ymin+ymax)/2.
81      E_min = (ymin*Omega_c*hbarc*1.0E-15/c)*1000. ! min
              photon energy in keV
          E_max = (ymax*Omega_c*hbarc*1.0E-15/c)*1000. ! max
              photon energy in keV
          E_cent =(y_cent*Omega_c*hbarc*1.0E-15/c) ! photon energy
              in MeV
          xLwg = 0.0135 ! pole length in m
          dTheta = xLwg/R_bend ! horizontal angular range

```

```

86      ij=2
      ik=1
      ift=1
      do ii=1,48
          if(E_cent.lt.xheeng(ii).and.ift.eq.1)then
91              ij=ii
              ik=ii-1
              ift=ift+1
          endif
      enddo
96      xrayabs=xhemu(ik)+
> ((E_cent-xheeng(ik))/(xheeng(ij)-xheeng(ik)))*
> (xhemu(ij)-xhemu(ik))
c      absconst=0.023*(2./4.)*(2.*xlambda_c*1.0E+10/y_cent)
**2.78
c      if (absconst.lt.0.1) absconst=0.1
101 c      write(6,*)E_cent,xrayabs
      absconst=xrayabs*(5.9/1000.)
      Amut=(1.0-exp(-absconst**0.5))
c      write(6,*)'Wiggler B-field and pole lengths =',Bwg,xLwg
c      write(6,*)'boost, central freq and bend radius=',gamma,
      Omega_c,
106 c      1          R_bend
c      write(6,*)'vertical ang. range, min and max photon energy
      =',
c      1 dTheta, E_min, E_max,xlambda_c,absconst,y_cent,Amut,
      E_cent
c      Psi_min = -asin(1./gamma) ! min vertical angle
c      Psi_max = asin(1./gamma) ! max vertical angle
111 c      alpha_min = gamma*Psi_min ! boosted min vertical angle
c      alpha_max = gamma*Psi_max ! boosted max vertical angle
c      z_min = (ymin/2.)*(1.+alpha_min**2.)*1.5 ! z=(y/2)*(1+
alpha)^1.5
c      z_max = (ymax/2.)*(1.+alpha_max**2.)*1.5
c      write(6,*)alpha_min,alpha_max,z_min,z_max
116 c      xNe=xIe*1.0E-06/qe ! # of electrons
      xi=1.5*gamma**2*hbarc*1.0E-15/xMe/R_bend ! crit
      parameter
      xHbyHo=gamma*hbarc*1.0E-15/xMe/R_bend
      tau=(8.*sqrt(3.)/15.)*(hbarc*1.0E-15/xMe/c) ! use hbarc/
      qe^2 =137
1      *(1./xHbyHo)**3*(1./gamma**2.)*137.0
121 c      sflip=hbarc*(xLwg/c)*(1.+8.*sqrt(3.)/15.)*0.5*1./tau
c      write(6,*)'sflip probability',sflip
      const1=3.*xNe*gamma*dTheta/(4.*pi**2.*137.)
      const2=4.*const1*xi
c      call p3pgs(ymin,ymax,n1,fn01,gn01,vint1) ! integrations
      for N
126 c      call p3pgs(ymin,ymax,n2,fn02,gn02,vint2) ! integraton
      for Delta N
      xn=const1*vint1
      dn=const2*vint2

```

```

      xa=(dn/xn)*sqrt(2.*xn)
      xpow=xn*E_cent*1.6E-19*1.0E+6! power released in W
131      dpow1=dn*E_cent*1.6E-19*1.0E+10 ! power of spin light in
           W
C      write(6,*)'edep',xdpow !Ebeam,gamma,dTheta,gamma*dTheta,
const1,vint1
C      write(6,*)'photon energy, #of photons, up/dn diff, assym,
C      1 analyzing pwr, photons abs'
C      write(6,15)(E_min+E_max)/2000.,xn,dn,dn/xn,xa,xpow,Amut*
xn
136 C      y_cent = E/E_max (do not add), E_cent: bi central energy(
do not add), xn: tot. num. events (add),dn:Events from Spin
light(add), dn/xn = ratio, xa= events above - events below/
sum, xpow: integrated per bin, Amut*xn: signal size
           couxn = couxn + xn
           coudn = coudn + dn
           enddo
           xn = couxn
           dn = coudn
141      write(10,15)y_cent,E_cent,xn,dn,dn/xn,xa,xpow,Amut*xn
           ymin=ymax
           enddo
           close (10)
146 15  format(1x,f6.3,1x,f6.3,1x,e15.3,1x,e15.3,1x,e15.3,1x,e15
           .3,1x,
           1      e15.3,1x,e15.3)
           END

SUBROUTINE IKV(V,X,VM,BI,DI,BK,DK)
151 C
C      =====
C      Purpose: Compute modified Bessel functions Iv(x) and
C      Kv(x), and their derivatives
C      Input : x --- Argument ( x > 0 )
C      v --- Order of Iv(x) and Kv(x)
156 C      ( v = n+v0, n = 0,1,2,..., 0 < v0 < 1 )
C      Output: BI(n) --- In+v0(x)
C      DI(n) --- In+v0'(x)
C      BK(n) --- Kn+v0(x)
161 C      DK(n) --- Kn+v0'(x)
C      VM --- Highest order computed
C      Routines called:
C      (1) GAMMA for computing the gamma function
C      (2) MSTA1 and MSTA2 to compute the starting
166 C      point for backward recurrence
C      =====
C
C      IMPLICIT DOUBLE PRECISION (A-H,O-Z)
C      DIMENSION BI(0:*),DI(0:*),BK(0:*),DK(0:*)
171 PI=3.141592653589793D0
      X2=X*X
      N=INT(V)

```

```

V0=V-N
IF (N.EQ.0) N=1
176 IF (X.LT.1.0D-100) THEN
    DO 10 K=0,N
        BI(K)=0.0D0
        DI(K)=0.0D0
        BK(K)=-1.0D+300
181 10 DK(K)=1.0D+300
        IF (V.EQ.0.0) THEN
            BI(0)=1.0D0
            DI(1)=0.5D0
        ENDIF
186 VM=V
        RETURN
    ENDIF
PIV=PI*V0
VT=4.0D0*V0*V0
191 IF (V0.EQ.0.0D0) THEN
    A1=1.0D0
    ELSE
        V0P=1.0D0+V0
        CALL GAMMA(V0P,GAP)
196 A1=(0.5D0*X)**V0/GAP
    ENDIF
K0=14
IF (X.GE.35.0) K0=10
IF (X.GE.50.0) K0=8
201 IF (X.LE.18.0) THEN
    BI0=1.0D0
    R=1.0D0
    DO 15 K=1,30
        R=0.25D0*R*X2/(K*(K+V0))
206 BI0=BI0+R
        IF (DABS(R/BI0).LT.1.0D-15) GO TO 20
15 CONTINUE
20 BI0=BI0*A1
    ELSE
211 CA=DEXP(X)/DSQRT(2.0D0*PI*X)
        SUM=1.0D0
        R=1.0D0
        DO 25 K=1,K0
            R=-0.125D0*R*(VT-(2.0D0*K-1.0D0)**2.0)/(K*X)
216 25 SUM=SUM+R
            BI0=CA*SUM
        ENDIF
M=MSTA1(X,200)
IF (M.LT.N) THEN
221 N=M
    ELSE
        M=MSTA2(X,N,15)
    ENDIF
F2=0.0D0

```

```

226      F1=1.0D-100
      DO 30 K=M,0,-1
          F=2.0D0*(V0+K+1.0D0)/X*F1+F2
          IF (K.LE.N) BI(K)=F
          F2=F1
231 30    F1=F
      CS=BI0/F
      DO 35 K=0,N
35        BI(K)=CS*BI(K)
      DI(0)=V0/X*BI(0)+BI(1)
236 40    DO 40 K=1,N
40        DI(K)=-(K+V0)/X*BI(K)+BI(K-1)
      IF (X.LE.9.0D0) THEN
          IF (V0.EQ.0.0D0) THEN
241            CT=-DLOG(0.5D0*X)-0.5772156649015329D0
            CS=0.0D0
            W0=0.0D0
            R=1.0D0
            DO 45 K=1,50
246              W0=W0+1.0D0/K
              R=0.25D0*R/(K*K)*X2
              CS=CS+R*(W0+CT)
              WA=DABS(CS)
              IF (DABS((WA-WW)/WA).LT.1.0D-15) GO TO 50
45            WW=WA
251 50    BK0=CT+CS
      ELSE
          V0N=1.0D0-V0
          CALL GAMMA(V0N,GAN)
          A2=1.0D0/(GAN*(0.5D0*X)**V0)
256          A1=(0.5D0*X)**V0/GAP
          SUM=A2-A1
          R1=1.0D0
          R2=1.0D0
          DO 55 K=1,120
261            R1=0.25D0*R1*X2/(K*(K-V0))
            R2=0.25D0*R2*X2/(K*(K+V0))
            SUM=SUM+A2*R1-A1*R2
            WA=DABS(SUM)
            IF (DABS((WA-WW)/WA).LT.1.0D-15) GO TO 60
266 55    WW=WA
60        BK0=0.5D0*PI*SUM/DSIN(PIV)
      ENENDIF
      ELSE
          CB=DEXP(-X)*DSQRT(0.5D0*PI/X)
271          SUM=1.0D0
          R=1.0D0
          DO 65 K=1,K0
65            R=0.125D0*R*(VT-(2.0*K-1.0)**2.0)/(K*X)
            SUM=SUM+R
276          BK0=CB*SUM
      ENENDIF

```

```

BK1=(1.0D0/X-BI(1)*BK0)/BI(0)
BK(0)=BK0
BK(1)=BK1
281 DO 70 K=2,N
      BK2=2.0D0*(V0+K-1.0D0)/X*BK1+BK0
      BK(K)=BK2
      BK0=BK1
70    BK1=BK2
286 DK(0)=V0/X*BK(0)-BK(1)
80    DO 80 K=1,N
      DK(K)=- (K+V0)/X*BK(K)-BK(K-1)
VM=N+V0
RETURN
291 END

SUBROUTINE GAMMA(X,GA)
C
C
296 C =====
C Purpose: Compute gamma function a(x)
C Input : x --- Argument of a(x)
C          ( x is not equal to 0, -1, -2,uuu)
C Output: GA --- a(x)
C
301 C =====
C

IMPLICIT DOUBLE PRECISION (A-H,O-Z)
DIMENSION G(26)
PI=3.141592653589793D0
306 IF (X.EQ.INT(X)) THEN
      IF (X.GT.0.0D0) THEN
311 10    GA=1.0D0
          M1=X-1
          DO 10 K=2,M1
            GA=GA*K
          ELSE
            GA=1.0D+300
          ENDIF
      ELSE
316    IF (DABS(X).GT.1.0D0) THEN
          Z=DABS(X)
          M=INT(Z)
          R=1.0D0
          DO 15 K=1,M
321 15    R=R*(Z-K)
          Z=Z-M
          ELSE
            Z=X
          ENDIF
326    DATA G/1.0D0,0.5772156649015329D0,
&         -0.6558780715202538D0, -0.420026350340952D-1,
&         0.1665386113822915D0, -.421977345555443D-1,
&         -.96219715278770D-2, .72189432466630D-2,

```

```

331 &      -.11651675918591D-2, -.2152416741149D-3,
&      .1280502823882D-3, -.201348547807D-4,
&      -.12504934821D-5, .11330272320D-5,
&      -.2056338417D-6, .61160950D-8,
&      .50020075D-8, -.11812746D-8,
336 &      .1043427D-9, .77823D-11,
&      -.36968D-11, .51D-12,
&      -.206D-13, -.54D-14, .14D-14, .1D-15/
      GR=G(26)
20      DO 20 K=25,1,-1
          GR=GR*Z+G(K)
341      GA=1.0D0/(GR*Z)
          IF (DABS(X).GT.1.0D0) THEN
              GA=GA*R
              IF (X.LT.0.0D0) GA=-PI/(X*GA*DSIN(PI*X))
          ENDIF
346      ENDIF
          RETURN
          END

351      INTEGER FUNCTION MSTA1(X,MP)
C
C      =====
C      Purpose: Determine the starting point for backward
C              recurrence such that the magnitude of
356 C              Jn(x) at that point is about 10^(-MP)
C      Input :  x      --- Argument of Jn(x)
C              MP     --- Value of magnitude
C      Output:  MSTA1 --- Starting point
C      =====
361 C

          IMPLICIT DOUBLE PRECISION (A-H,O-Z)
          A0=DABS(X)
          N0=INT(1.1*A0)+1
          F0=ENVJ(N0,A0)-MP
366          N1=N0+5
          F1=ENVJ(N1,A0)-MP
          DO 10 IT=1,20
              NN=N1-(N1-N0)/(1.0D0-F0/F1)
              F=ENVJ(NN,A0)-MP
371          IF(ABS(NN-N1).LT.1) GO TO 20
              N0=N1
              F0=F1
              N1=NN
          10      F1=F
376          20      MSTA1=NN
          RETURN
          END

381      INTEGER FUNCTION MSTA2(X,N,MP)

```

```

C
C
C =====
C Purpose: Determine the starting point for backward
C recurrence such that all Jn(x) has MP
386 C significant digits
C Input : x --- Argument of Jn(x)
C n --- Order of Jn(x)
C MP --- Significant digit
C Output: MSTA2 --- Starting point
391 C =====
C
C IMPLICIT DOUBLE PRECISION (A-H,O-Z)
C A0=DABS(X)
C HMP=0.5D0*MP
396 C EJN=ENVJ(N,A0)
C IF (EJN.LE.HMP) THEN
C OBJ=MP
C N0=INT(1.1*A0)
C ELSE
401 C OBJ=HMP+EJN
C N0=N
C ENDIF
C F0=ENVJ(N0,A0)-OBJ
C N1=N0+5
406 C F1=ENVJ(N1,A0)-OBJ
C DO 10 IT=1,20
C NN=N1-(N1-N0)/(1.0D0-F0/F1)
C F=ENVJ(NN,A0)-OBJ
C IF (ABS(NN-N1).LT.1) GO TO 20
411 C N0=N1
C F0=F1
C N1=NN
10 C F1=F
20 C MSTA2=NN+10
416 C RETURN
C END
C
C REAL*8 FUNCTION ENVJ(N,X)
C DOUBLE PRECISION X
421 C ENVJ=0.5D0*DLOG10(6.28D0*N)-N*DLOG10(1.36D0*X/N)
C RETURN
C END
C
426 C SUBROUTINE P3PGS ( A, B, N, FN, GN, VINT )
C
C *****72
C
C THIS SUBROUTINE USES THE PRODUCT TYPE THREE-POINT GAUSS-
431 C LEGENDRE-SIMPSON RULE COMPOUNDED N TIMES TO APPROXIMATE

```

```

C THE INTEGRAL FROM A TO B OF THE FUNCTION FN(X) * GN(X).
C FN AND GN ARE FUNCTION SUBPROGRAMS WHICH MUST BE SUPPLIED
C BY THE USER. THE RESULT IS STORED IN VINT.
C
436   DOUBLE PRECISION A, AG, AM(2,3), B, F(2), FN, G(3),
      & GN, H, VINT, X(2), Y(2), DBLE

      DATA AM(1,1), AM(2,3) / 2 * 1.718245836551854D0 /,
      & AM(1,2), AM(2,2) / 2 * 1.D0 /, AM(1,3), AM(2,1)
441   & / 2 * -.2182458365518542D0 /

      H = ( B - A ) / DBLE ( FLOAT ( N ) )
      X(1) = A + .1127016653792583D0 * H
      X(2) = A + .8872983346207417D0 * H
446   Y(1) = A + H / 2.D0
      Y(2) = A + H
      VINT = 0.D0
      G(3) = GN ( A )
      DO 3 I = 1, N
451   AG = FN ( Y(1) )
      G(1) = G(3)
      DO 1 J = 1, 2
      F(J) = FN ( X(J) )
      G(J+1) = GN ( Y(J) )
456   X(J) = X(J) + H
      Y(J) = Y(J) + H
      VINT = VINT + AG * 4.D0 * G(2)
      DO 3 J = 1, 2
461   AG = 0.D0
      DO 2 K = 1, 3
      AG = AG + AM(J,K) * G(K)
      VINT = VINT + F(J) * AG
466   VINT = H * VINT / 9.D0

      RETURN
      END

471   function fn01(x)
      implicit none

      integer n

476   double precision fn01
      double precision x

      fn01 = x

481   return
      end

```

```

function fn02(x)
implicit none
486
integer n

double precision fn02
double precision x
491

fn02 = x**2.

return
end
496

function gn01(x)
implicit real*8(A-H,O-Z)

c   real*8 Psi_min,Psi_max,alpha_min,alpha_max,y,vint3
501 c   real*8 gamma

c   integer n
external fn03
external gn03

506 c   double precision gn01
c   double precision x

parameter (n=20)

511 common gamma,y

Psi_min = -asin(1./gamma) ! min vertical angle
Psi_max = asin(1./gamma) ! max vertical angle
516 alpha_min = 2.*gamma*Psi_min ! boosted min vertical angle
alpha_max = 2.*gamma*Psi_max ! boosted max vertical angle
alpha_cutoffm=-0.16
alpha_cutoffp=0.16
y=x
521 call p3pgs(alpha_min,alpha_max,n,fn03,gn03,vint31)
c   call p3pgs(alpha_min,alpha_cutoffm,n,fn03,gn03,vint31)
c   call p3pgs(alpha_cutoffp,alpha_max,n,fn03,gn03,vint32)
gn01 = vint31 !+vint32

526 return
end

function gn02(x)
implicit none

531 real*8 Psi_min,Psi_max,alpha_min,alpha_max,y,vint4
real*8 gamma

integer n

```

```
536     external fn04
      external gn04

      double precision gn02
      double precision x
541     parameter (n=20)
      common gamma,y

      Psi_min = -asin(1./gamma) ! min vertical angle
      Psi_max = asin(1./gamma) ! max vertical angle
546     alpha_min = 0. !16 !for the diff the int is from
           alpha_cutoff to alpha_max
      alpha_max = 2.*gamma*Psi_max ! boosted max vertical angle
      y=x
      call p3pgs(alpha_min,alpha_max,n,fn04,gn04,vint4)
      gn02 = vint4

551
      return
      end

      function fn03(x)
556     implicit none

      integer n

561     double precision fn03
      double precision x

      fn03 = (1+x**2.)**2.

566     return
      end

      function fn04(x)
571     implicit none

      integer n

576     double precision fn04
      double precision x

      fn04 = x*(1+x**2.)**1.5

581     return
      end

      function gn03(x)
586     implicit real*8 (A-H,O-Z)
```

```

c      real*8 z,v,k23,k13,gamma,y,vm
c      dimension BI(0:*),DI(0:*),BK(0:*),DK(0:*)

591 c      integer n

      double precision gn03
      double precision x
      common gamma,y
596 COMMON BI(0:250),DI(0:250),BK(0:250),DK(0:250)

      xk23=0.
      xk13=0.
      z=(y/2.)*(1+x**2)**1.5 ! z= (omega/2omega_c)*(1+alpha^2)
          ^3/2
601 c      write(6,*)'gn03 gamma,y,x,z',gamma,y,x,z
      v=2./3.
      CALL IKV(V,z,VM,BI,DI,BK,DK)
      xk23=BK(0)

606      v=1./3.
      CALL IKV(V,z,VM,BI,DI,BK,DK)
      xk13=BK(0)
c      write(6,*)'g03 k23 k13',xk23,xk13
      gn03 = xk23**2. + x**2.*xk13**2/(1+x**2.)
611
      return
      end

616 function gn04(x)
      implicit real*8(A-H,0-Z)

c      real*8 z,v,k23,k13,y,vm,gamma
c      Dimension BI(0:*),DI(0:*),BK(0:*),DK(0:*)

621 c      integer n

c      double precision gn04
c      double precision x
      Common gamma,y
626 COMMON BI(0:250),DI(0:250),BK(0:250),DK(0:250)

      z=(y/2.)*(1+x**2)**1.5
      v=2./3.
      CALL IKV(V,z,VM,BI,DI,BK,DK)
631      xk23=BK(0)

      v=1./3.
      CALL IKV(V,z,VM,BI,DI,BK,DK)
      xk13=BK(0)

636      gn04 = xk23*xk13

```

```

return
end

```

B.2 LANL POISSON SUPEFISH GEOMETRY DESCRIPTION

Listing 2: LANL Poisson Input

```

Dipole Magnet Problem
DIPOLE 6 Simulation of Spin Light Chicane Magnet

4 ; Copyright 1987, by the University of California.
  ; Unauthorized commercial use is prohibited.
  ; Author: Prajwal Mohanmurthy; Dec, 2011; (prajwal@jlab.org)

&reg kprob=0,      ! Poisson or Pandira problem
9 mode=0,         ! Some materials have variable permeability
nbsup=0,         ! added by gbf !
nbslf=0,
rhogam=0.001     !try this gbf
xreg1=10.0,kreg1=82,! Physical and logical coordinates of x
14 xreg2=25.0,kreg2=98,
xreg3=48.0,kreg3=150,

yreg1=14.0,lreg1=65,! Y line regions
yreg2=18.0,lreg2=70,
19 yreg3=21.0,lreg3=74,
lmax=80 &

&po x= -30.0000,y= 0.0000 &
&po x=60.000,y= 0.0000&
24 &po x=60.000,y=30.0000 &
&po x= -30.0000,y=30.0000 &
&po x= -30.0000,y= 0.0000 &

&reg mat=1,cur=-1040000.0 &
29 &po x=30.5000,y=6.000 &
&po x=40.0000,y=6.000 &
&po x=40.0000,y=12.000 &
&po x=30.5000,y=12.000 &
&po x=30.5000,y=6.000 &

34 &reg mat=1,cur=1040000.0 &
&po x=-10.0000,y=6.000 &
&po x=-0.5000,y=6.000 &
&po x=-0.5000,y=12.000 &
39 &po x=-10.000,y=12.000 &
&po x=-10.000,y=6.000 &

&reg mat=3,mtid=-2, mshape=0 &
&po x= 0.00,y= 5.62 &

```

```
44 &po x= 1.50,y= 2.62 &
    &po x= 3.50,y= 1.27 &
    &po x=26.50,y= 1.27 &
    &po x=28.50,y= 2.65 &
    &po x=30.00,y= 5.62 &
49 &po x=30.00,y= 12.50 &
    &po x=40.50,y= 12.60 &
    &po x=40.50,y= 0.00 &
    &po x=60.00,y= 0.00 &
    &po x=60.00,y= 30.00 &
54 &po x= 0.00,y= 30.00 &
    &po x= 0.00,y= 5.62 &

    &mt mtid=1
    bgam=0.00000 0.0017513135
59 900 0.001747079
    950 0.001741742
    1000 0.001735498
    1050 0.001728309
    1100 0.00172014
64 1150 0.001710963
    1200 0.001700753
    1250 0.001689494
    1300 0.001677174
    1350 0.001663786
69 2800 0.001080694
    2850 0.001068051
    2900 0.001056142
    2950 0.001044912
    3000 0.001034309
74 3050 0.001024289
    3100 0.001014809
    3150 0.001005828
    3200 0.000997312
    3250 0.000989226
79 3300 0.000981539
    3350 0.000974222
    4000 0.000904952
    4500 0.000856798
    5000 0.000818493
84 5500 0.000788085
    6000 0.000764202
    6500 0.000745863
    7000 0.000732376
    7500 0.000723261
89 8000 0.000718209
    8500 0.000717054
    9000 0.000719758
    9500 0.000726411
    10000 0.000737231
94 10500 0.000752594
    10578 0.0007562580
```

	11319	0.0007951022
	11940	0.0008375209
	12451	0.0008834703
99	12912	0.0009293680
	13313	0.0009764671
	13654	0.0010253255
	13935	0.0010764263
	14216	0.0011254924
104	14447	0.0011767475
	14618	0.0012313603
	14789	0.0012846865
	15020	0.0013315579
	15131	0.0013879251
109	15252	0.0014423770
	15432	0.0014912019
	15594	0.0015389351
	15705	0.0015918497
	16180	0.0018542555
114	16840	0.0023752969
	17150	0.0029154519
	17360	0.0034566194
	17620	0.0039729837
	17830	0.0044863167
119	18200	0.0054945055
	18950	0.0079176564
	19500	0.0102564103
	20200	0.0148588410
	20650	0.0193798450
124	20950	0.0238663484
	21600	0.0370370370
	21900	0.0456621005
	23000	0.0869565217
	23386	0.1002810000
129	23850	0.1181630000
	24408	0.1387420000
	25079	0.1622460000
	25885	0.1888580000
	26854	0.2186950000
134	28019	0.2517840000 &

B.3 RECURSIVE SR SPECTRA ADDING CODE

Listing 3: Mathematica7

```

!Recurssive SR - Spectra Adding Code
!Author: Prajwal Mohanmurthy, Dec 2011 (prajwal@jlab.org)
! Mathematica 7 File
up=30;
5 down=25;
  asym=5;
  sigup=up/E;

```

```

sigdown=down/E;
width=200; (*100+100*)
10 mid=width/2;
motion=10;
scale=0;
If[up-asy! = down,Print["Check Var : asym, down, up"]]
sr=Table[Table[0,{k,1,width+(2 motion)},{kk,1,21}]; (*Set 'X'
width =21*)
15 (*Print["-----"];*)
For[xx=1,xx<=21,xx++,
count=0;
count2=0;
x=xx-1;
20 For[y=0,If[x<=10,y<= x,y<=10-Abs[10-x] ],y++,
count++;
(*Print[x, ":x | y:",y];*)
For[k=motion+1+y,k<=motion+mid+y,k++,
sr[[xx]][[k]]+=Floor[(down*E^(-((x-10)^2+(y)^2)/sigdown))]];
25 scale+=E^(-((x-10)^2+(y)^2)/sigdown);
(*Print["Adding ",Floor[(down*E^(-((x-10)^2+(y)^2)/sigdown))]], "
to ",k];*)
];
For[k=motion+mid+1+y,k<=motion+width+y,k++,
sr[[xx]][[k]]+=Floor[(up*E^(-((x-10)^2+(y)^2)/sigup ))]];
30 scale+=E^(-((x-10)^2+(y)^2)/sigdown);
(*Print["Adding ",Floor[(up*E^(-((x-10)^2+(y)^2)/sigup ))]], " to
",k];*)
];
];
(*Print["-----"];*)
35 For[y=0,If[x<= 10,y< x,y<10-Abs[10-x] ],y++,
count2++;
(*Print[x, ":x | y:",-(y+1)];*)
For[k=motion+1+-(y+1),k<=motion+mid-(y+1),k++,
sr[[xx]][[k]]+=Floor[(down*E^(-((x-10)^2+(y+1)^2)/sigdown))]];
40 scale+=E^(-((x-10)^2+(y)^2)/sigdown);
(*Print["Adding ",Floor[(down*E^(-((x-10)^2+(y+1)^2)/sigdown))
], " to ",k];*)
];
For[k=motion+mid+1-(y+1),k<=motion+width-(y+1),k++,
sr[[xx]][[k]]+=Floor[(up*E^(-((x-10)^2+(y+1)^2)/sigup ))]];
45 scale+=E^(-((x-10)^2+(y)^2)/sigdown);
(*Print["Adding ",Floor[(up*E^(-((x-10)^2+(y+1)^2)/sigup ))]], "
to ",k];*)
];
];
(*Print["-----"];*)
50 (*Print[count,"\t",count2,"\t",count+count2];*)
(*Print["-----"];*)
];
N[scale]
(*ListPlot3D[sr,PlotRange->Full]*)

```

```

55 400.023
    nsize=520;
    nwm=nsize-(2*motion);
    Dimensions[sr];
    sr2=Table[Table[0,{k,1,220}},{k,1,nsize}];
60 Dimensions[sr2]
    Dimensions[sr2];
    For[i2=1,i2<=21,i2++,
    For[j2=1,j2<=220,j2++,
    For[k2=i2,k2<nwm+i2,k2++,
65 sr2[[k2]][[j2]]+=sr[[i2]][[j2]];
    ];
    ];
    ];
    Export["3dcontour_manypt.png",ListPlot3D[Transpose[sr2],
        ColorFunction->"BlueGreenYellow",AxesLabel->{"x","y","N"},
        PlotRange->Full]]
70 {520,220}
    3dcontour_manypt.png
    sr3=Table[Table[0,{k,1,220}},{k,1,nsize}];
    Dimensions[sr3];
    For[i2=11,i2<=110,i2++,
75 For[j2=11,j2<=nwm+motion,j2++,
    sr3[[j2]][[i2]]=sr2[[nsize/4]][[50]];
    ];
    ];
    For[i2=111,i2<=210,i2++,
80 For[j2=11,j2<=nwm+motion,j2++,
    sr3[[j2]][[i2]]=Max[sr2];
    ];
    ];
    Export["3dcontour_onept2.png",ListPlot3D[Transpose[sr3],AxesLabel
        ->{"x","y","N"},ColorFunction->"BlueGreenYellow",PlotRange->
        Full]]
85 3dcontour_onept2.png
    Clear[write2]
    write2=OpenWrite["srXYdisc1.dat"]
    WriteString[write2,"# x (micro m)" ,"|" ,"y (micro m)" ,"|" ,"N" ,"\\
        n"];
    For[i=1,i<=220,i++,
90 For[j=1,j<=nsize,j++,
    WriteString[write2,Floor[20 j] ,"\\t" ,Floor[5 i] ,"\\t" ,Floor[sr2
        [[j]][[i]]] ,"\\n"];
    ];
    ];
    Close[write2]
95 OutputStream[srXYdisc1.dat,36]
    srXYdisc1.dat
    Clear[write1]
    write1=OpenWrite["srXYdiscone1.dat"]
    WriteString[write1,"# x (micro m)" ,"|" ,"y (micro m)" ,"|" ,"N" ,"\\
        n"];

```

```

100 For[i=1,i<=220,i++,
    For[j=1,j<=nsize,j++,
        WriteString[writel,Floor[20 j] ,"\t" ,Floor[5 i],"\t",Floor[sr3
            [[j]][[i]]],"\n"];
    ];
]
105 Close[writel]
    OutputStream[srXYdiscone1.dat,37]
srXYdiscone1.dat

```

For the complete program, refer to mohanmurthy.com/a/SpinIC.gz.tar

B.4 GEANT4 GEOMETRY FILE

Listing 4: GEANT4 Toolkit - SpinIC executable

```

////////////////////////////////////
// Author      : Prajwal Mohanmurthy, 09/2012      //
3 //              (prajwal@mohanmurthy.com)        //
//              Mississippi State University, MS 39762, USA//
// Description : Creates 2 X IC at z = +5.m        //
//              3 X Wigglers at z = -5.m          //
//              5 X Collimators on faces of magnets//
8 //              Dipole_B_Field = 4T              //
//              Energy(e- beam) = 11GeV           //
//              e- Gun Position at z = -5.1m       //
////////////////////////////////////

13 #include "SpinICDetectorConstruction.hh"
#include "G4Material.hh"
#include "G4Box.hh"
#include "G4Tubs.hh"
#include "G4LogicalVolume.hh"
18 #include "G4PVPlacement.hh"
#include "G4VisAttributes.hh"

#include "G4FieldManager.hh"
#include "G4UniformMagField.hh"
23 #include "G4Mag_UsualEqRhs.hh"
#include "G4ClassicalRK4.hh"
#include "G4ChordFinder.hh"

#include "G4NistManager.hh"
28

// Constructor
SpinICDetectorConstruction::SpinICDetectorConstruction()
: fCheckOverlaps(false)
33 //verbosity(0)
{ }

// Destructor
SpinICDetectorConstruction::~SpinICDetectorConstruction()

```

```

38 { }

// Materials
void SpinICDetectorConstruction::DefineMaterials()
{
43 // Get nist material manager
G4NistManager* nistManager = G4NistManager::Instance();

nistManager->FindOrBuildMaterial("G4_Galactic");
nistManager->FindOrBuildMaterial("G4_Fe");
48 nistManager->FindOrBuildMaterial("G4_Al");
nistManager->FindOrBuildMaterial("G4_Ar");
nistManager->FindOrBuildMaterial("G4_Pb");
// Print materials
G4cout << *(G4Material::GetMaterialTable()) << G4endl;
53 }

G4VPhysicalVolume* SpinICDetectorConstruction::Construct()
{
// Materials
58 DefineMaterials();

// World
G4double worldSizeXY = 2.*m;
63 G4double worldSizeZ = 20.*m;
G4Material* worldMaterial = G4Material::GetMaterial("
G4_Galactic");

G4VSolid* solidWorld
= new G4Box("World", //
its name
68 worldSizeXY/2, worldSizeXY/2, worldSizeZ/2); //
its size

flogicalWorld
= new G4LogicalVolume(
73 solidWorld, // its solid
worldMaterial, // its material
"World"); // its name

G4VPhysicalVolume* physicalWorld
= new G4PVPlacement(
78 0, // no rotation
G4ThreeVector(), // at (0,0,0)
flogicalWorld, // its logical volume
"World", // its name
0, // its mother volume
83 false, // no boolean operation
0, // copy number
fCheckOverlaps); // checking overlaps

```

```

88 // World Visualization attributes
//
G4VisAttributes* worldVisAtt = new G4VisAttributes(G4Colour
    (1.0,1.0,1.0));
worldVisAtt->SetVisibility(true);
worldVisAtt->SetForceWireframe(true);
flogicalWorld->SetVisAttributes(worldVisAtt);
93
// Define Everything else
DefineMagnets();
DefineIC();
98
// Always return physical volume of world
return physicalWorld;
}
103
void SpinICDetectorConstruction::DefineMagnets()
{
//Magnet Materials
G4Material* magnetIron = G4Material::GetMaterial("G4_Fe");
108 G4Material* magnetVacuum = G4Material::GetMaterial("
    G4_Galactic");
G4Material* magnetColl = G4Material::GetMaterial("G4_Pb");

// ***** Magnets: 1 - 3 *****

113 // Strength of field
G4double stdfield = 4.0*tesla;

// Magnet Geometry Parameters
G4double magnetPlateThickness = 5.*cm;
118 G4double magnetPlateSeparation = 10.*cm;
G4double magnetXSize = 10.*cm;
G4double magnetSmallZsize = 10.*cm;
G4double magnetLargeZsize = 2.*magnetSmallZsize;

123 // Magnet Positions
G4double magnet1ZPos = -5.05*m;
G4double magnet2ZPos = -6.7*m;
G4double magnet3ZPos = -8.35*m;

128
// ***** 2 Small Magnets - Magnets 1&3 *****

// Define small magnet outer volume as large block of iron
G4Box* smallMagnetOuter
133 = new G4Box("s_smallMagnet_outer", // its name
    magnetXSize/2,
    (magnetPlateThickness*2.+magnetPlateSeparation)
    /2,

```

```

        magnetSmallZsize/2);           // its size

138  G4LogicalVolume* logicalSmallMagnetOuter
    = new G4LogicalVolume(smallMagnetOuter, // its solid
                          magnetIron,     // its
                          material        // its
                          "l_smallMagnet_outer"); // its name

143  // Define small magnet inner volume as block of vacuum
    G4Box* smallMagnetInner
    = new G4Box("s_smallMagnet_inner", // its name
               magnetXSize/2,
               magnetPlateSeparation/2,
148  magnetSmallZsize/2);           // its size

    G4LogicalVolume* logicalSmallMagnetInner
    = new G4LogicalVolume(smallMagnetInner, // its solid
                          magnetVacuum,    // its
                          material        // its
                          "l_smallMagnet_inner"); // its name

    // Place Inner magnet volume as a daughter of outer magnet
    // volume
158  new G4PVPlacement(0, // no rotation
                     G4ThreeVector(), // at (0,0,0) in
                     outer volume    // its logical
                     logicalSmallMagnetInner, // its logical
                     "pv_smallMagnet_inner", // its name
                     logicalSmallMagnetOuter, // ** its mother
                     volume **
                     false, // no boolean
163  operation // operation
                     0, // copy number
                     fCheckOverlaps); // checking
                     overlaps

    // Place small magnet twice, this will include outer and
    // inner
168  // 1st magnet

    #if 1
    new G4PVPlacement(0, // no
                      rotation
                      G4ThreeVector(0.,0.,magnet1ZPos), //
                      position
                      logicalSmallMagnetOuter, // its logical
                      volume
173  "pv_Magnet1", // its name
                      flogicalWorld, // its mother
                      volume

```

```

        false,                // no boolean
        operation
    0,                        // copy number
    fCheckOverlaps);        // checking
    overlaps
178 #endif

    // 3rd magnet

183 #if 1
    new G4PVPlacement(0,                // no
        rotation
        G4ThreeVector(0.,0.,magnet3ZPos), //
        position
        logicalSmallMagnetOuter, // its logical
        volume
        "pv_Magnet3",                // its name
        flogicalWorld,                // its mother
        volume
        false,                        // no boolean
        operation
    0,                        // copy number
    fCheckOverlaps);        // checking
    overlaps
188 #endif

193 // ***** Large Magnet - Magnet 2 *****

198 // Define large magnet outer volume as large block of iron
G4Box* largeMagnetOuter
= new G4Box("s_largeMagnet_outer",    // its name
    magnetXSize/2,
    (magnetPlateThickness*2.+magnetPlateSeparation)
    /2,
203    magnetLargeZsize/2);           // its size

G4LogicalVolume* logicalLargeMagnetOuter
= new G4LogicalVolume(largeMagnetOuter, // its solid
    magnetIron,                // its
    material
208    "l_largeMagnet_outer"); // its name

// Define large magnet inner volume as block of vacuum
G4Box* largeMagnetInner
= new G4Box("s_largeMagnet_inner",    // its name
    magnetXSize/2,
    magnetPlateSeparation/2,
213    magnetLargeZsize/2);           // its size

```

```

218 G4LogicalVolume* logicalLargeMagnetInner
= new G4LogicalVolume(largeMagnetInner,      // its solid
                      magnetVacuum,        // its
                      material
                      "l_largeMagnet_inner"); // its name
223
// Place Inner magnet volume as a daughter of outer magnet
// volume
new G4PVPlacement(0,                          // no rotation
                  G4ThreeVector(),          // at (0,0,0) in
                  outer volume
                  logicalLargeMagnetInner,  // its logical
                  volume
228 "pv_largeMagnet_inner", // its name
                  logicalLargeMagnetOuter, // ** its mother
                  volume **
                  false,                    // no boolean
                  operation
                  0,                        // copy number
                  fCheckOverlaps);        // checking
                  overlaps
233
// Place Large magnet, this will include inner and outer
#if 1
new G4PVPlacement(0,                          // no
                  rotation
238 G4ThreeVector(0.,0.,magnetZZPos), //
                  position
                  logicalLargeMagnetOuter,   // its
                  logical volume
                  "pv_Magnet2",             // its name
                  flogicalWorld,           // its mother
                  volume
                  false,                    // no boolean
                  operation
243 0,                        // copy number
                  fCheckOverlaps);        // checking
                  overlaps
#endif
248 // **** Magnetic Fields ****
// Create magnetic fields and managers
//Field in +Y
G4UniformMagField* magFieldUp
253 = new G4UniformMagField(G4ThreeVector(0.,stdfield,0.));
G4FieldManager* localFieldManagerUp = new G4FieldManager();
localFieldManagerUp->SetDetectorField(magFieldUp);

```

```

localFieldManagerUp->CreateChordFinder(magFieldUp);
// Assign to small magnets
258 logicalSmallMagnetInner->SetFieldManager(localFieldManagerUp,
      true);

//Field in -Y
G4UniformMagField* magFieldDown
= new G4UniformMagField(G4ThreeVector(0.,-1.*stdfield,0.));
263 G4FieldManager* localFieldManagerDown = new G4FieldManager();
localFieldManagerDown->SetDetectorField(magFieldDown);
localFieldManagerDown->CreateChordFinder(magFieldDown);
// Assign to large magnet
logicalLargeMagnetInner->SetFieldManager(
268     localFieldManagerDown, true);

// Magnet Visualization attributes
//
273 G4VisAttributes* outerMagVisAtt = new G4VisAttributes(
      G4Colour(0.0, 0.0, 1., 0.5));
outerMagVisAtt->SetVisibility(true);
outerMagVisAtt->SetForceSolid(true);
logicalLargeMagnetOuter->SetVisAttributes(outerMagVisAtt);
logicalSmallMagnetOuter->SetVisAttributes(outerMagVisAtt);

278     G4VisAttributes* innerMagVisAtt = new G4VisAttributes(
      G4Colour(1.0, 1.0, 1.0, 0.3));
innerMagVisAtt->SetVisibility(true);
innerMagVisAtt->SetForceSolid(true);
logicalLargeMagnetInner->SetVisAttributes(innerMagVisAtt);
283 logicalSmallMagnetInner->SetVisAttributes(innerMagVisAtt);

//
*****

//***** Collimators Geometries *****
// | | |
288 // | | |
// | | *\
// | * | \
// * | | \
// | | |---\collTheta angle
293 // * | |
// | * |
// | | *
// | | |
// | | |

298 G4double collPlateX = magnetXSize;
G4double collPlateY = (magnetPlateThickness*2.+
      magnetPlateSeparation);

```

```

303      //***** Collimators *****

      //*****! Main Collimators on Magnet faces !*****

308      //!Attn: MANUAL INPUT
      G4double collThetaAngle1 = 0.01;//Angle subtended by
           collimator to its serving magnet's center
      G4double outerRadius = 0.5*mm;    //radius of the beam
           hole
      G4double collPlateZ = 10.0*mm;    //Collimator Thickness

313      // Hole for beam
      G4double innerRadius = 0.*cm;
      G4double collHoleHz = collPlateZ;
      G4double startAngle = 0.*deg;
      G4double spanningAngle = 360.*deg;

318      G4Tubs* collHole
           = new G4Tubs("coll_hole",
                       innerRadius,
                       outerRadius,
323                       collHoleHz,
                       startAngle,
                       spanningAngle);

      G4LogicalVolume* logicalCollHole
328      = new G4LogicalVolume(collHole,    // its solid
                              magnetVacuum, // its
                              material
                              "l_coll_hole"); // its name

           //##### MagnetNumber = 1, forward #####

333      // Define 5mm block of Pb
      G4Box* collBlockm1f
           = new G4Box("coll_block_m1f",    // its name
                       collPlateX/2,
338                       collPlateY/2,
                       collPlateZ/2);    // its size

      G4LogicalVolume* logicalCollBlockm1f
           = new G4LogicalVolume(collBlockm1f, // its solid
                              magnetColl,    // its
                              material
                              "l_coll_block_m1f"); // its name

           //{Hole,Slits} at MagnetNumber = 1, forward: Placement

348      //Hole

```

```

new G4PVPlacement(0, // no rotation
                  G4ThreeVector(), // at (0,0,0) in
                    outer volume
                  logicalCollHole, // its logical volume
353 "pv_coll_block_m1f", // its name
                  logicalCollBlockm1f, // ** its mother
                    volume **
                  false, // no boolean
                    operation
                  0, // copy number
                  fCheckOverlaps); // checking
358 overlaps

// Collimator Slits
G4double collSlitWm1f1 = 0.06125*cm; //slit width
363 of the collimator

G4Box* collSlitm1f1
= new G4Box("coll_block_m1f1", // its name
           collSlitWm1f1/2,
           collPlateY/2,
368 collPlateZ/2); // its size

G4LogicalVolume* logicalCollSlitm1f1
= new G4LogicalVolume(collSlitm1f1, // its solid
                      magnetVacuum, // its
                        material
373 "l_coll_slit_m1f1"); // its name

G4double collSlitWm1f2 = 0.125*cm; //slit width
of the collimator

G4Box* collSlitm1f2
378 = new G4Box("coll_block_m1f2", // its name
           collSlitWm1f2/2,
           collPlateY/2,
           collPlateZ/2); // its size

G4LogicalVolume* logicalCollSlitm1f2
383 = new G4LogicalVolume(collSlitm1f2, // its solid
                      magnetVacuum, // its
                        material
                        "l_coll_slit_m1f2"); // its name

388 //Slits
new G4PVPlacement(0, // no rotation

```

```

393         G4ThreeVector(collThetaAngle1*(magnet1ZPos-
            magnet3ZPos+(magnetSmallZsize/2))
            ,0.,0.),
            logicalCollSlitm1f1, // its logical volume
            "pv_coll_slit_m1f1", // its name
            logicalCollBlockm1f, // ** its mother
            volume **
            false, // no boolean
            operation
            0, // copy number
            fCheckOverlaps); // checking
            overlaps
398
            new G4PVPlacement(0, // no
                rotation
                G4ThreeVector(collThetaAngle1*(magnet1ZPos-
                    magnet2ZPos+(magnetSmallZsize)),0.,0.),
                logicalCollSlitm1f2, // its logical volume
                "pv_coll_slit_m1f2", // its name
                logicalCollBlockm1f, // ** its mother
                volume **
                false, // no boolean
                operation
                0, // copy number
                fCheckOverlaps); // checking
                overlaps
403
408 //MagnetNumber = 1, forward: Placement

            new G4PVPlacement(0, // no
                rotation
413         G4ThreeVector(0.,0.,magnet1ZPos+((
            magnetSmallZsize/2)+(collPlateZ/2))),
            logicalCollBlockm1f, // its logical volume
            "pv_coll_slit_m1f", // its name
            flogicalWorld, // ** its mother volume **
            false, // no boolean
            operation
418         0, // copy number
            fCheckOverlaps); // checking
            overlaps

423 #if 1
            ##### MagnetNumber = 1, Backward #####

            // Define 5mm block of Pb
            G4Box* collBlockm1b
            = new G4Box("coll_block_m1b", // its name
                collPlateX/2,
428         collPlateY/2,

```

```

        collPlateZ/2);          // its size

G4LogicalVolume* logicalCollBlockm1b
= new G4LogicalVolume(collBlockm1b,      // its solid
433      magnetColl,                  // its
        material
        "l_coll_block_m1b"); // its name

    //{Hole,Slits} at MagnetNumber = 1, Backward: Placement
438 //Hole

new G4PVPlacement(0,                // no rotation
    G4ThreeVector(1.0*mm,0.,0.),    // at
        (0,0,0) in outer volume
    logicalCollHole, // its logical volume
443 "pv_coll_block_m1b", // its name
    logicalCollBlockm1b, // ** its mother
        volume **
    false,                // no boolean
        operation
    0,                    // copy number
    fCheckOverlaps);     // checking
448 overlaps

    // Collimator Slits
    G4double collSlitWm1b1 = 0.25*cm; //slit width
        of the collimator

G4Box* collSlitm1b1
453 = new G4Box("coll_block_m1b1", // its name
    collSlitWm1b1/2,
    collPlateY/2,
    collPlateZ/2); // its size

G4LogicalVolume* logicalCollSlitm1b1
458 = new G4LogicalVolume(collSlitm1b1, // its solid
    magnetVacuum, // its
        material
        "l_coll_slit_m1b1"); // its name

463 G4double collSlitWm1b2 = 0.25*cm; //slit width
        of the collimator

G4Box* collSlitm1b2
468 = new G4Box("coll_block_m1b2", // its name
    collSlitWm1b2/2,
    collPlateY/2,
    collPlateZ/2); // its size

G4LogicalVolume* logicalCollSlitm1b2
= new G4LogicalVolume(collSlitm1b2, // its solid

```

```

473         magnetVacuum,           // its
            material
            "l_coll_slit_m1b2"); // its name

    //Slits
478 new G4PVPlacement(0,           // no rotation
                    G4ThreeVector(collThetaAngle1*(magnet1ZPos-
                        magnet3ZPos-(magnetSmallZsize/2))
                        ,0.,0.),
                    logicalCollSlitm1b1, // its logical volume
                    "pv_coll_slit_m1b1", // its name
                    logicalCollBlockm1f, // ** its mother
                        volume **
                    false,           // no boolean
                        operation
483 0,                               // copy number
                    fCheckOverlaps); // checking
                        overlaps

    new G4PVPlacement(0,           // no
        rotation
                    G4ThreeVector(collThetaAngle1*(magnet1ZPos-
                        magnet2ZPos),0.,0.),
488 logicalCollSlitm1b2, // its logical volume
                    "pv_coll_slit_m1b2", // its name
                    logicalCollBlockm1b, // ** its mother
                        volume **
                    false,           // no boolean
                        operation
493 0,                               // copy number
                    fCheckOverlaps); // checking
                        overlaps

    //MagnetNumber = 1, Backward: Placement

498 new G4PVPlacement(0,           // no
        rotation
                    G4ThreeVector(0.,0.,magnet1ZPos-((
                        magnetSmallZsize/2)+(collPlateZ/2))),
                    logicalCollBlockm1b, // its logical volume
                    "pv_coll_slit_m3f", // its name
503 flogicalWorld, // ** its mother volume **
                    false,           // no boolean
                        operation
                    0,               // copy number
                    fCheckOverlaps); // checking
                        overlaps

508 //##### MagnetNumber = 2, forward #####

```

```

    // Define 5mm block of Pb
G4Box* collBlockm2f
513 = new G4Box("coll_block_m2f",           // its name
              collPlateX/2,
              collPlateY/2,
              collPlateZ/2);             // its size

G4LogicalVolume* logicalCollBlockm2f
518 = new G4LogicalVolume(collBlockm2f,    // its solid
                          magnetColl,     // its
                          material
                          "l_coll_block_m2f"); // its name

    // {Hole, Slits} at MagnetNumber = 2, forward: Placement

    // Hole

new G4PVPlacement(0,                       // no rotation
528   G4ThreeVector(16.80*mm, 0., 0.),
      // 16.59515*mm
      logicalCollHole, // its logical volume
      "pv_coll_block_m2f", // its name
      logicalCollBlockm2f, // ** its mother
      volume **
      false, // no boolean
533   operation
      0, // copy number
      fCheckOverlaps); // checking
      overlaps

    // Collimator Slits
G4double collSlitWm2f1 = 0.25*cm; // slit width
538   of the collimator

G4Box* collSlitm2f1
= new G4Box("coll_block_m2f1",           // its name
            collSlitWm2f1/2,
            collPlateY/2,
543   collPlateZ/2); // its size

G4LogicalVolume* logicalCollSlitm2f1
= new G4LogicalVolume(collSlitm2f1,    // its solid
                      magnetVacuum,    // its
                      material
548   "l_coll_slit_m2f1"); // its name

G4double collSlitWm2f2 = 0.25*cm; // slit width
      of the collimator

G4Box* collSlitm2f2
553 = new G4Box("coll_block_m2f2",           // its name

```



```

593         flogicalWorld, // ** its mother volume **
        false,           // no boolean
            operation
        0,               // copy number
        fCheckOverlaps); // checking
            overlaps

598     //##### MagnetNumber = 2, backward #####

        // Define 5mm block of Pb
G4Box* collBlockm2b
603 = new G4Box("coll_block_m2b",           // its name
            collPlateX/2,
            collPlateY/2,
            collPlateZ/2);                 // its size

G4LogicalVolume* logicalCollBlockm2b
608 = new G4LogicalVolume(collBlockm2b,    // its solid
            magnetColl,                    // its
            material
            "l_coll_block_m2b");          // its name

        //{{Hole,Slits} at MagnetNumber = 2, backward: Placement
613 //Hole

        new G4PVPlacement(0,               // no rotation
            G4ThreeVector(16.80*mm,0.,0.),
            //16.59515*mm
618         logicalCollHole, // its logical volume
            "pv_coll_block_m2b", // its name
            logicalCollBlockm2b, // ** its mother
            volume **
            false,                 // no boolean
            operation
        0,                         // copy number
623         fCheckOverlaps);        // checking
            overlaps

        // Collimator Slits
        G4double collSlitWm2b = 0.25*cm; //slit width
            of the collimator

628 G4Box* collSlitm2b
        = new G4Box("coll_block_m2b",     // its name
            collSlitWm2b/2,
            collPlateY/2,
            collPlateZ/2);               // its size

633 G4LogicalVolume* logicalCollSlitm2b
        = new G4LogicalVolume(collSlitm2b, // its solid

```

```

        magnetVacuum,          // its
            material
        "l_coll_slit_m2b"); // its name
638
//Slits
new G4PVPlacement(0,          // no
    rotation
        G4ThreeVector(collThetaAngle1*(magnet2ZPos-
            magnet3ZPos-(2.*magnetSmallZsize/2))
            ,0.,0.),
        logicalCollSlitm2b, // its logical volume
643    "pv_coll_slit_m2b", // its name
        logicalCollBlockm2b, // ** its mother
            volume **
        false,              // no boolean
            operation
        0,                  // copy number
        fCheckOverlaps); // checking
648    overlaps

//MagnetNumber = 2, backward: Placement

new G4PVPlacement(0,          // no
    rotation
653    G4ThreeVector(0.,0.,magnet2ZPos - ((2.*
        magnetSmallZsize/2)+(collPlateZ/2))),
        logicalCollBlockm2b, // its logical volume
        "pv_coll_slit_m2b", // its name
        flogicalWorld, // ** its mother volume **
        false,           // no boolean
            operation
658    0,                  // copy number
        fCheckOverlaps); // checking
            overlaps

//##### MagnetNumber = 3, forward #####
663
// Define 5mm block of Pb
G4Box* collBlockm3f
= new G4Box("coll_block_m3f", // its name
    collPlateX/2,
668    collPlateY/2,
        collPlateZ/2); // its size

G4LogicalVolume* logicalCollBlockm3f
= new G4LogicalVolume(collBlockm3f, // its solid
673    magnetColl, // its
        material
        "l_coll_block_m3f"); // its name

```

```

    //Hole,Slits} at MagnetNumber = 3, forward: Placement
678 //Hole

new G4PVPlacement(0, // no rotation
                  G4ThreeVector(1.*mm,0.,0.),
                  logicalCollHole, // its logical volume
683 "pv_coll_block_m3f", // its name
                  logicalCollBlockm3f, // ** its mother
                  volume **
                  false, // no boolean
                  operation
                  0, // copy number
                  fCheckOverlaps); // checking
                  overlaps

688 // Collimator Slits
G4double collSlitWm3f = 0.25*cm; //slit width
    of the collimator

G4Box* collSlitm3f
693 = new G4Box("coll_block_m3f", // its name
              collSlitWm3f/2,
              collPlateY/2,
              collPlateZ/2); // its size

698 G4LogicalVolume* logicalCollSlitm3f
    = new G4LogicalVolume(collSlitm3f, // its solid
                          magnetVacuum, // its
                          material
                          "l_coll_slit_m3f"); // its name

703 //Slits
new G4PVPlacement(0, // no
                  rotation
                  G4ThreeVector(collThetaAngle1*((
                              magnetSmallZsize/2)),0.,0.),
                  logicalCollSlitm3f, // its logical volume
708 "pv_coll_slit_m3f", // its name
                  logicalCollBlockm3f, // ** its mother
                  volume **
                  false, // no boolean
                  operation
                  0, // copy number
                  fCheckOverlaps); // checking
                  overlaps

713 //MagnetNumber = 3, forward: Placement

new G4PVPlacement(0, // no
                  rotation

```

```

718         G4ThreeVector(0.,0.,magnet3ZPos + ((
            magnetSmallZsize/2)+(collPlateZ/2))),
            logicalCollBlockm3f, // its logical volume
            "pv_coll_slit_m3f", // its name
            flogicalWorld, // ** its mother volume **
            false, // no boolean
                operation
723         0, // copy number
            fCheckOverlaps); // checking
                overlaps

#endif

728 }

void SpinICDetectorConstruction::DefineIC()
{
733 #if 1
            // Define the IC geometry here

            //IC Geometry Parameters
            G4double icXysize = 12.*cm;
738         G4double icZsize = 1.0*m;
            G4double icShellThick = 1.*mm;
            G4double icWinXysize = 20.*cm;

            //IC Position
743         G4double icPosZ = 5.5*m; /*Y = 0*/
            G4double icPosX = (icXysize/2.) + (4.*cm); /*Depends on
                icXysize*/

            //materials
            G4Material* icShell = G4Material::GetMaterial("G4_Al");
748         G4Material* icGas = G4Material::GetMaterial("G4_Ar");
            G4Material* icPb = G4Material::GetMaterial("G4_Pb");

            // Define icOuter volume as large block of Al
            G4Box* icOuter
753         = new G4Box("s_ic_Outer", // its name
                (icXysize + (icShellThick*2.))/2.,
                (icXysize + (icShellThick*2.))/2.,
                (icZsize + (icShellThick*2.))/2.);
                // its size

758         G4LogicalVolume* logicalIcOuter
            = new G4LogicalVolume(icOuter, // its solid
                icShell, // its material
                "l_ic_Outer"); // its name

763         // Define icInner volume as block of Ar

```

```

G4Box* icInner
= new G4Box("s_ic_Inner",          // its name
            (icXysize)/2.,
            (icXysize)/2.,
768          (icZsize)/2.);          // its size

G4LogicalVolume* logicalIcInner
= new G4LogicalVolume(icInner,    // its solid
                      icGas,      // its material
773                      "l_ic_Inner"); // its name

    // Define icWin volume as block of Ar
G4Box* icWin
= new G4Box("s_ic_Win",          // its name
            (icWinXysize)/2.,
778          (icWinXysize)/2.,
            (icShellThick)/2.);  // its size

G4LogicalVolume* logicalIcWin
= new G4LogicalVolume(icWin,      // its solid
                      icGas,      // its material =
783                      {icGas, icPb}
                      "l_ic_Win"); // its name

    // Place icInner volume as a daughter of icOuter volume
788 new G4PVPlacement(0,          // no rotation
                    G4ThreeVector(), // at (0,0,0) in
                    outer volume
                    logicalIcInner, // its logical volume
                    "pv_ic_merge",  // its name
                    logicalIcOuter, // ** its mother volume **
793                    false,        // no boolean
                    operation
                    0,              // copy number
                    fCheckOverlaps); // checking
                    overlaps

    // Place icWin volume as a daughter of icOuter volume
798 new G4PVPlacement(0,          // no rotation
                    G4ThreeVector(0.,0.,-(icZsize +
                    icShellThick)/2.), // at (x,y,z) in
                    outer volume
                    logicalIcWin,   // its logical volume
                    "pv_ic_merge_win", // its name
                    logicalIcOuter, // ** its mother volume **
803                    false,        // no boolean
                    operation
                    0,              // copy number
                    fCheckOverlaps); // checking
                    overlaps

    // Physically Place icInner + icOuter combo volume

```

```

808 #if 1
      new G4PVPlacement(0, // no
        rotation
            G4ThreeVector(-icPosX,0.,icPosZ), //
            position
            logicalIcOuter, // its logical
            volume
813 "pv_ic1", // its name
            flogicalWorld, // its mother
            volume
            false, // no boolean
            operation
            0, // copy number
            fCheckOverlaps); // checking
            overlaps
818 #endif

      new G4PVPlacement(0, // no
        rotation
            G4ThreeVector(icPosX,0.,icPosZ), //
            position
823 logicalIcOuter, // its logical
            volume
            "pv_ic2", // its name
            flogicalWorld, // its mother
            volume
            false, // no boolean
            operation
            0, // copy number
828 fCheckOverlaps); // checking
            overlaps

      // IC Visualization attributes
      //
      G4VisAttributes* innerICVisAtt = new G4VisAttributes(G4Colour
        (0.7, 0.7, 0.5, 1.0));
833 innerICVisAtt->SetVisibility(true);
      innerICVisAtt->SetForceSolid(true);
      logicalIcInner->SetVisAttributes(innerICVisAtt);

      #if 1
838 G4VisAttributes* outerICVisAtt = new G4VisAttributes(G4Colour
        (0.0, 0.5, 0.5, 0.5));
      outerICVisAtt->SetVisibility(true);
      outerICVisAtt->SetForceSolid(true);
      logicalIcOuter->SetVisAttributes(outerICVisAtt);
      #endif
843 #endif

```

```
}

```

B.5 GEANT4 STACKING ACTION FILE

Listing 5: GEANT4 Toolkit - SpinIC executable

```

////////////////////////////////////
2 // Author      : Prajwal Mohanmurthy, 09/2012      //
//              (prajwal@mohanmurthy.com)          //
//              Mississippi State University, MS 39762, USA//
// Description : Implements assymetry              //
//              Counts SR + SL Photons vs. Energy   //
7 //////////////////////////////////////////////////

#include "SpinICStackingAction.hh"
#include "SpinICAnalysis.hh"
#include "G4ProcessType.hh"
12 #include "G4VProcess.hh"
#include "G4Track.hh"
#include "Randomize.hh"
#include "G4Pow.hh"
#include <time.h>
17

SpinICStackingAction::SpinICStackingAction()
{
    G4cout << "***** Stacking Action Created *****"
            << G4endl;
22 }

SpinICStackingAction::~SpinICStackingAction()
{
27 }

G4ClassificationOfNewTrack SpinICStackingAction::ClassifyNewTrack
(const G4Track * track)
{
    G4int PDG = track->GetParticleDefinition()->GetPDGEncoding();
32 G4int parentID = track->GetParentID();
G4int trackID = track->GetTrackID();
G4int stepNum = track->GetCurrentStepNumber();

    G4int icnum = 3; //(1: Left IC, 2: right IC)
37 G4int MagnetNumber = 0;
G4ThreeVector Pos = track->GetPosition();

    G4double genenergy = track->GetKineticEnergy()/MeV;
G4double chrg = track->GetParticleDefinition()->GetPDGCharge
    ();
42 G4double prodtm = track->GetGlobalTime();

```

```

G4int prodstm = time(NULL);

if (PDG == 22) {
    if (Pos.z()/m > -5.2 && Pos.z()/m < -4.9) {MagnetNumber =
        1;}
47     else if (Pos.z()/m > -6.85 && Pos.z()/m < -5.55) {
        MagnetNumber = 2;}
    else if (Pos.z()/m > -8.5 && Pos.z()/m < -8.2) {
        MagnetNumber = 3;}
    else {MagnetNumber = 5;}
}

52 // Get the creator process of the track that deposits energy
const G4VProcess* edepCreatorProcess = track->
    GetCreatorProcess();
G4ProcessType creatorProcessType = fNotDefined;
G4int creatorProcessSubType = 0;
if(edepCreatorProcess)
57 {
    //edepCreatorProcess->DumpInfo();
    creatorProcessType = edepCreatorProcess->GetProcessType()
        ;
    creatorProcessSubType = edepCreatorProcess->
        GetProcessSubType();
}
62 G4int cpTypeCode = (G4int)creatorProcessType*10000 +
    creatorProcessSubType;

#if 1
G4double phasymmetry = (4.543E-7) + (0.0000572046*genergy) +
    (-0.0000306751*std::pow(genergy,2)) + (0.0000138074*std:::
    pow(genergy,3)) + (-3.37522E-6*std::pow(genergy,4)) +
    (3.29347E-7*std::pow(genergy,5));
G4double asymmetry = 1. - phasymmetry;
67 //G4double asymmetry = 1.;

//up-down asymmetry
if (MagnetNumber==1 || MagnetNumber==3)
{
72     if (track->GetMomentumDirection().y() < 0. &&
        G4UniformRand() < asymmetry) {return fKill;}
}
else if (MagnetNumber==2)
{
77     if (track->GetMomentumDirection().y() > 0. &&
        G4UniformRand() < asymmetry) {return fKill;}
}
//Energy Spread asym
if (G4UniformRand() > phasymmetry) {return fKill;}*/
82 #endif

// Determine which IC based on xyz-position

```

```
87   if (((Pos.z()/m >= 4.4) && (Pos.z()/m <= 6.6)) && ((Pos.y()/m
      >=-0.225) && (Pos.y()/m <= 0.225)))
    {
      //icnum = 4;
      if ((Pos.x()/m >= -0.36) && (Pos.x()/m <= 0.0)){ icnum =
        1; }
      else if ((Pos.x()/m <= 0.36) && (Pos.x()/m >=
        0.0)){ icnum = 2; }
    }
92   if(icnum==2 /*PDG==22 && genergy > 0.465 && parentID<=1000*/)
    {
      // Get AnalysisManager to fill ntuples/histograms
      G4AnalysisManager* analysisManager = G4AnalysisManager::
        Instance();
97   analysisManager->FillNtupleDColumn(0, genergy);

      analysisManager->FillNtupleDColumn(1, Pos.x()/m);
      analysisManager->FillNtupleDColumn(2, Pos.y()/m);
102  analysisManager->FillNtupleDColumn(3, Pos.z()/m);

      analysisManager->FillNtupleDColumn(4, chrg);
      analysisManager->FillNtupleIColumn(5, PDG);
      analysisManager->FillNtupleIColumn(6, parentID);
107  analysisManager->FillNtupleIColumn(7, cpTypeCode);
      //analysisManager->FillNtupleDColumn(8, prodtm);
      analysisManager->FillNtupleIColumn(8, MagnetNumber);
      analysisManager->FillNtupleIColumn(9, trackID);

112  analysisManager->AddNtupleRow();
    }
    return fUrgent;
  }
```